IEEE Access
Multidisciplinary ⋮ Rapid Review ⋮ Open Access Journal

Received 28 March 2024, accepted 11 April 2024, date of publication 16 April 2024, date of current version 26 April 2024.

Digital Object Identifier 10.1109/ACCESS.2024.3389979

TOPICAL REVIEW

AI-Enhanced Gas Flares Remote Sensing and Visual Inspection: Trends and Challenges

MUAZ AL RADI[1], PENGFEI LI[1], SAID BOUMARAF[1], JORGE DIAS[1], (Senior Member, IEEE), NAOUFEL WERGHI[1], (Senior Member, IEEE), HAMAD KARKI[2], AND SAJID JAVED[1]

[1]Department of Electrical Engineering and Computer Science, Khalifa University, Abu Dhabi, United Arab Emirates
[2]Department of Mechanical Engineering, Khalifa University, Abu Dhabi, United Arab Emirates

Corresponding authors: Muaz Al Radi (100059660@ku.ac.ae) and Pengfei Li (Pengfei.leen@outlook.com)

This work was supported by Khalifa University and Abu Dhabi National Oil Company (ADNOC) through the project "Advanced Deep Learning Systems for Monitoring And Analyzing Flare Activities in Video Data" under Grant ADNOC-21110553.

ABSTRACT The real-time analysis of gas flares is one of the most challenging problems in the operation of various combustion-involving industries, such as oil and gas refineries. Despite the crucial role of gas flares in securing safe plant operation and lowering environmental pollution, they are among the least monitored components of petrochemical plants due to their harsh working environments. Remote sensing techniques are emerging as potential alternatives for conventional sampling-based techniques in visual inspection and performance analysis. This paper presents an in-depth review of significant achievements in Gas flares monitoring over past two decades and highlights ongoing challenges in Artificial Intelligence (AI)-enhanced remote inspection. By reading the content, both industry professionals and academic researchers can gain a comprehensive knowledge of improvements from the integration of AI and remote sensing, understanding the trend of Gas flares monitoring. The paper commences with an analysis of RGB camera-based methods, focusing on how their combination with cutting-edge machine learning and deep learning algorithms can significantly improve the detection, segmentation, and measurement of gas flare systems. It then explores the use of hyper-spectral imaging techniques, including infrared cameras and space-borne satellite sensors, underscoring their potential in remote monitoring and performance analysis. Additionally, the effectiveness of multi-view inspection methods is assessed, highlighting how these approaches enhance the monitoring capabilities. Finally, the paper identifies key research areas that require further attention. It also presents a clearer direction for future progress, emphasizing the importance of continuous research to foster advancements and facilitate broader commercial adoption.

INDEX TERMS Remote sensing, AI-enhanced visual inspection, gas flares monitoring, hyper-spectral imaging, deep learning.

I. INTRODUCTION

Petrochemical fuels, such as oil and natural gas, are among the most important energy resources worldwide in various types of sectors, like transportation, process industries, and power production [1], [2]. Recognizing the huge amount of oil production and consumption, robust safety considerations are increasingly desired to be included in refineries and petrochemical plants.

In every oil refinery and petrochemical plant, the flare stack plays a crucial role in ensuring the safe operation of the plant under abnormal conditions and minimizing the amount of harmful gases released to the atmosphere. The flare stack burns the excess gas that results from various defects in the plant's operation, such as water shortage, gas shortage, power shutdown, and equipment failure. This burning largely reduces the negative environmental effects of exhaust gas by converting harmful methane, carbon monoxide, and other large carbon compounds to safe water vapor and carbon dioxide. Despite its important role in the plant's operation, the flare stack is one of the least monitored components and

The associate editor coordinating the review of this manuscript and approving it for publication was Gerardo Di Martino.

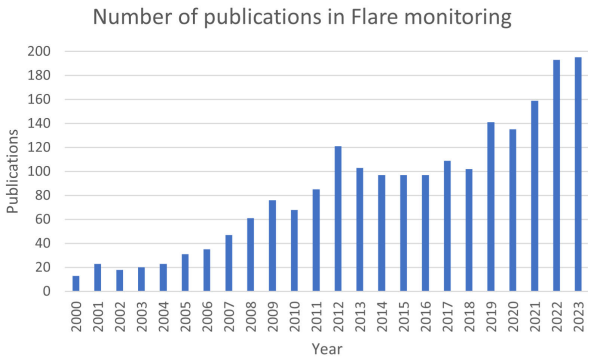

FIGURE 1. The increasing number of publications in gas flaring and its analysis from 2000 to 2023, data obtained using Google Scholar advanced search.

its operation is hard to regulate. This is due to the combustion condition that takes place in open air, at very high temperatures, and in high elevations. Inadequate monitoring of the flare system results in slow detection of abnormal flare operation which results in the release of hazardous gases to the environment and may lead to deadly fires and explosions. Contact monitoring of the flare system's operation is extremely difficult due to the highly corrosive and hot combustion environment. This makes remote monitoring of the flare's operation using remote sensing cameras and other optical sensors a high potential alternative for real-time monitoring and regulation [1].

An excellent flare remote sensing system should satisfy several requirements [3]. First, it should provide sufficiently accurate measures that can be relied on to reflect the actual flare's performance. Both qualitative and quantitative flare performance measures should be accurately evaluated so that the flare's operation can be easily assessed. Second, it should have low equipment and operation costs so that it can be easily adopted worldwide. Third, it should be implemented in a way that does not interfere with the operation of other plant components. By looking at these requirements, remote monitoring using visual sensors emerges as an excellent option for both real-time and scheduled monitoring of combustion flares [4], [5], [6], [7].

There has been a growing interest in the analysis of combustion flares in the last few years. Fig. 1 shows the increasing number of publications related to gas flaring and its inspection. In this work, the progress done on the application of various vision-based inspection techniques for the monitoring of combustion flares is reviewed. Few surveys on various aspects of flare monitoring are available in literature [8], [9]. However, our work is the first to comprehensively cover all aspects of vision-based inspection of flare systems, including RGB imaging, hyperspectral imaging, and multi-view inspection. A taxonomy of the progress done on vision-based inspection of combustion flares is shown in Fig. 2. A chronological overview of the most important flare analysis works throughout the last 20 years is illustrated in Fig. 3.

By looking at the existing works in literature, the most significant contributions of this survey are summarized as follows:

- This is the first work to comprehensively cover all aspects of visual inspection of combustion flare systems, including RGB imaging, hyperspectral imaging, and multi-view inspection, and their analysis techniques, such as image processing, machine learning, and deep learning.
- This work focuses on the application of various visual sensing techniques specifically for combustion flare monitoring rather than all types of combustion-related applications.
- Comprehensive comparisons of the existing inspection techniques on the publicly available datasets are included (in Tables 3, and 4), with summaries, discussions, and potential future research direction.

The main contents of this work are as follows. Section II illustrates the publicly available datasets and the used flare quality inspection measures. measures. Section III summarizes the application of RGB imaging techniques for detection, segmentation, and measurement for combustion flares and the implementation of different RGB images analysis techniques, such as image processing, machine learning, and deep learning. Section IV presents a survey of the application of various hyperspectral imaging techniques for the monitoring of flare systems and flaring activities including the use of infrared cameras, spaceborne satellite sensors, and theoretical modelling of hyperspectral data. Section V reviews the application of multi-view imaging techniques for flare inspection. Section VI highlights some critical future research directions and perspectives for further improving this technology and pushing it closer to commercialization.

II. BACKGROUND

In this section, background aspects on vision-based inspection of flare stacks are included. The main quality measures that are commonly used in the inspection of gas flares and the publicly-available datasets that are used in literature are overviewed.

A. GAS FLARES QUALITY MEASURES

In order to acquire an accurate insight into the performance of the Gas flare, several qualitative and quantitative quality measures are used. Obtaining appropriate and accurate flare efficiency measures is a crucial step for improving the overall flare performance. In this section, quality measures that are commonly used for evaluating flare's performance are illustrated.

1) EXISTENCE OF FLAME [2], [10]

In recent studies, Al Radi et al. [2], [10] pointed out that "an important measure qualitative that must be considered when analyzing the performance of flares is the existence of visible flame from the flare pilot. If the flare pilot is

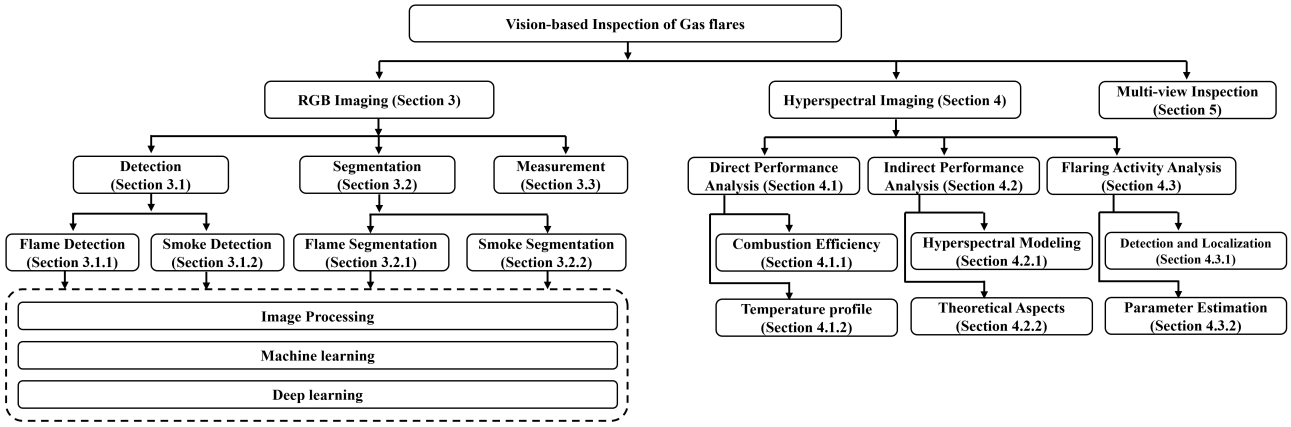

FIGURE 2. Taxonomy of visual inspection of flares.

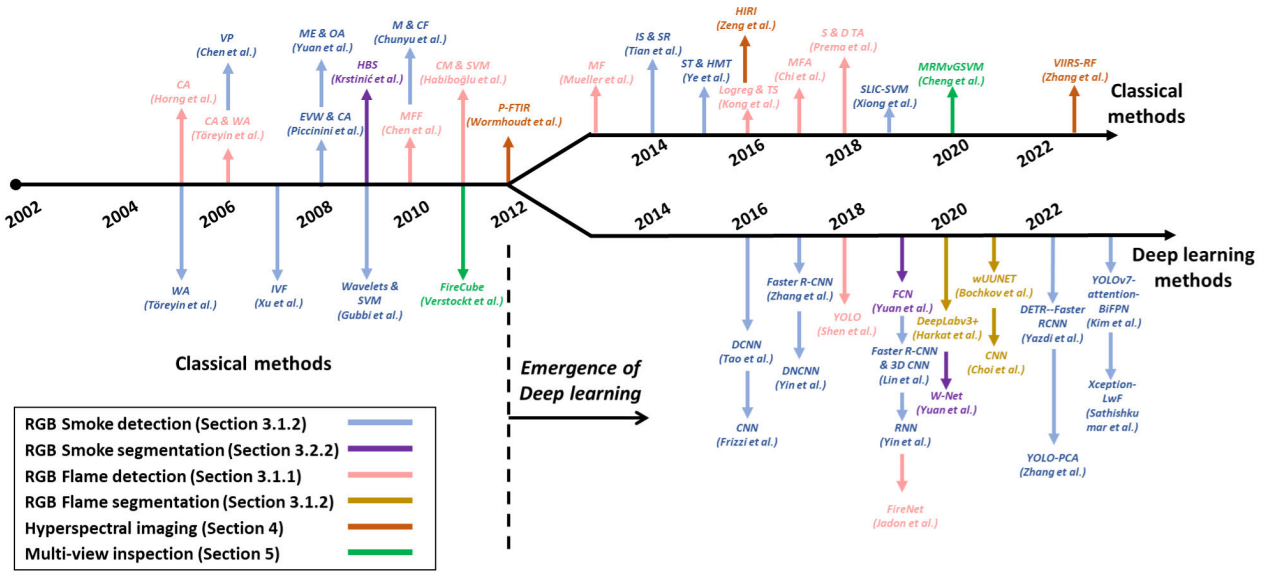

FIGURE 3. Chronological overview of the most important flare analysis works in the last 20 years.

working properly, it will ensure the combustion of the flared gases and their safe release to the environment. On the other hand, failures in the flare pilot system can result in major hazards due to abnormal operation such as dangerous gas leaks, fires, and explosions [11]. If the state of the flare pilot is not determined accurately and quickly during operation, abnormal operation will be hard to detect and mitigate. The proper operation of the flare pilot ensures that the flare system is ignited and is working efficiently. The ignition of the flare pilot can be observed visually through the existence of visible flame. Thus, the detection of flame is an important quality measure that must be considered when analyzing flare systems."

2) EXISTENCE AND QUANTIFICATION OF SMOKE/SOOT [10]

Referring to Al Radi, Li et al. [10]: "the release of smoke is an important measure to monitor in the operation of flare systems. As combustion flares convert the excess gas to carbon dioxide and water vapor, the released gases should be transparent in the ideal case. However, when other types of carbon compounds result from the incomplete combustion process, dark smoke can be observed clearly. Soot, which is a combination of various large carbonaceous compounds, results from cases of inefficient flare operation and has very hazardous effects on the environment. The density of soot emission is indicated by the darkness of the released smoke where darker smoke has a higher soot amount and vice versa. Thus, the detection of released smoke from the combustion flare is an effective indicator for incomplete combustion and harmful gas release to the environment."

3) COMBUSTION EFFICIENCY (CE)

The combustion efficiency is one of the most important quantitative quality measures of combustion flares. It indicates the

flare's performance in converting harmful carbon monoxide and other large hydrocarbons to safe carbon dioxide. The following equation is used to evaluate the combustion efficiency [12]:

$$CE(\%) = \frac{[C]_{CO_2}}{\sum_i n_i[C]_{HC_i} + [C]_{CO} + [C]_{CO_2}} \quad (1)$$

where $CE(\%)$ is the flares percentage combustion efficiency, $[C]$ is the mole fraction or the volumetric concentration of the specie in the flare's plume, CO and CO_2 subscripts refer to carbon monoxide and carbon dioxide, respectively, HC_i refers to the i-th produced unburned hydrocarbon, such as methane (CH_4), and n_i is the number of carbon atoms in the i-th produced unburned hydrocarbon. When there are no produced carbon monoxide and other hydrocarbon compounds, the flare's entire carbon emission will be only carbon dioxide and the combustion efficiency will be 100%. However, additional carbon compounds such as soot and methane are almost always present and must be taken into consideration. On the other hand, if the concentration of some compound is negligible compared to the other produced compounds, it can be omitted from the equation and an accurate flare efficiency estimate can still be obtained. For example, if the concentration of produced carbon monoxide is very small, Eq. 1 can be reduced as follows:

$$CE(\%) = \frac{[C]_{CO_2}}{\sum_i n_i[C]_{HC_i} + [C]_{CO_2}} \quad (2)$$

Detecting precursors of combustion instabilities has also been a hot topic of recent research. An example, the paper published by Cellier et al [13] proposed a method for detecting precursors of combustion instability. The authors investigated Convolutional Recurrent Neural Networks (CRNNs) and trained them on acoustic signals collected from a combustor to classify them as either stable or unstable. The approach involved processing the signals using a spectrogram, followed by a CRNN architecture that combines both convolutional and recurrent layers. The proposed method shows encouraging results with high accuracies in predicting the onset of combustion instability, making it a promising tool for early detection and real-time prevention of combustion instability.

B. DATASETS

There have been several datasets that were proposed in the literature for analyzing different aspects of combustion flares. Tables 1 and 2 show the most important datasets that are commonly used for evaluating flare analysis algorithms which include image and video datasets for detection and segmentation tasks evaluation. There are two main types of datasets that were used previously in literature. The first is video datasets that contain datasets designed for flame detection tasks, such as VisiFire [14], and others designed for smoke, such as Visor [15]. The second type is image datasets that contain separate images of the required object whether for flame detection, such as BoWFire [16], or for smoke detection, such as Yuan et al. [17]. Some of these image datasets were obtained by splitting frames from smoke/flame videos and collecting the images in positive and negative folders. There is also a very important trend in the use of these datasets is that datasets with similar type are combined together to provide a more comprehensive training and testing dataset. For example, Muhammad et al. [18] used a combination of Khan et al. [19] and Foggia et al. [20] datasets. However, there is a crucial problem in flame and smoke detection research is that there are no unified datasets on which all new proposed methods are tested. Because of that, it is hard to compare the performance of different techniques as the used datasets for training and testing are mostly different. Unified datasets for detection and segmentation are highly required as they will make accurate performance comparisons possible. Moreover, there are very limited publicly available datasets of multispectral or hyperspectral imagery of flame and smoke. A dataset that was proposed by Toulouse [21] includes a wide range of flame images, including some multispectral images in the Near-Infrared (NIR) region combined with their corresponding RGB images. However, more work on providing comprehensive multispectral and hyperspectral benchmarking datasets is crucial.

In the field of Gas Flares analysis, the lack of unified publicly-available datasets is mainly because none of the existing data sets can satisfy four important aspects: large scale, diverse, balanced, and up-to-date. For example, data sets like Visor [15] are more focused on smoke (which is regarded as an early indication of flare), so they contain more smoke instances than flare. On the other hand, some sets (like BoWFire [16]) are more interested in Flare event, so they collected the region of flare more. Besides, some researchers conducted their own Gas Flares experiments in a scale-down manner and therefore, collecting data sets in a near distance with simple background (such as white wall), this kind of data collection method may have limitations in simulating real Gas Flares scenario which is always a large-scale, background-mixed environment. Another issue results in the lack of benchmark data set is the inadequacy of up-to-date data sets. Starting from 2021, new technologies like CLIP (Contrastive Language-Image Pre-training) [22] are demonstrating its obvious improvement over previous image pattern detection model such as ViT (Vision Transformer) [23]. However, to use this text-image contrastive learning technique in analyzing Gas Flares, not only image instances of flare or soot are required, corresponding language prompts for each of these instances are also required. Unfortunately, in the current literature, no such data set is available. In the end of this data set section, the author is calling for collaborative efforts to develop a benchmark dataset that can include everyone to build up. This huge work can start with combining existing data sets like what Muhammad et al. [18] did in their work. This open benchmark building job is inspiring because once it is completed (even in its first version), different Gas Flares experiments can compare with

TABLE 1. Overview of the available video flame and smoke datasets.

Object	Dataset name	Positive videos	Negative videos	Total videos	Average resolution (W x H)	Year
Flame	CVPR-Lab-Fire [24]	8	8	16	320 x 240	2011
	VisiFire [14]	7	10	17	320 x 240	2012
	Foggia [20]	14	16	30	400 x 256	2015
Smoke	Visor [15]	15	0	15	320 x 240	2010

TABLE 2. Overview of the available image flame and smoke datasets.

Object	Dataset name	Positive images	Negative images	Total images	Average resolution (W x H)	Year
Flame	BoWFire [16]	119	107	226	1365 x 1024	2015
	FiSmo [25]	1604	3583	5,187	1024 x 768	2017
	Mlich [26]	1775	4611	6,386	1365 x 1024	2020
Smoke	Yuan [17]	4455	16874	21,329	320 x 240	2015
	Yin [27]	5695	18522	24,217	100 x 100	2017
	Xu [28]	35500	500	36000	256 x 256	2017
	FiSmo [25]	896	3583	4,479	1024 x 768	2017
	Khan [29]	18532	17774	36,306	640 x 360	2021

each other and the data set itself can also gradually become more large, diverse, balanced and up-to-date with upcoming technologies.

III. RGB IMAGING FOR COMBUSTION FLARE ANALYSIS

The basic and most important method for visual inspection of any structure is the use of RGB cameras. These cameras are advantageous in terms of their simple operation and produced data format. However, the highest effort in such inspection techniques is focused on the image analysis method that can produce useful information about the flare system using the RGB data. Obtained RGB images can be used in different modalities, such as detection, segmentation, and measurement. Detection algorithms can use RGB images to detect various flare-related objects, such as flame and smoke, and the detection can be used as a feedback signal for controlling the operation of the flare system. Similarly, image segmentation algorithms can be used to highlight the location of important objects in the observed flare image as it provides richer information about the detected object. Finally, the segmented smoke and flame pixel locations can be combined with detailed combustion mathematical models to measure important parameters of the flare's performance, such as the temperature distribution. In this section, the application of RGB imaging for detection, segmentation, and parameter measurement of combustion flare systems is reviewed and discussed.

A. DETECTION

In this subsection, the progress done on the detection of combustion-related object, namely flame and smoke, in gas flares scenes is summarized.

1) FLAME DETECTION

A study by Aslan et al. [30] implemented a novel Deep Convolutional Generative Adversarial Network (DCGAN) for detection of fire from video data. Their model utilizes the spatial and temporal characteristics of flame evolution throughout the video frames for achieving accurate flame detection. In order to extract the temporal characteristics of flame evolution, the values of pixels on the same vertical line were aligned with all other pixels falling on the same line from the other video frames so that evolution of flame throughout time is captured, a shown in Fig. 4 (a) and (b). Those temporal slices were collected and were used to train the generator and discriminator networks which are shown in Fig. 4 (c) and (d), respectively. Training was carried out in two steps. First, both the generator and discriminator networks are trained by giving a noise vector to the generator network and using the discriminator to distinguish between the generator's output and actual flame images, as shown in Fig. 4 (e). Next, the discriminator network is further trained alone using actual flame images and actual non-flame images, as shown in Fig. 4 (f). This training mechanism makes the DCGAN-based flame detector more robust compared to conventional CNN-based detectors. During testing, the discriminator network is used to distinguish flame-containing frames from non-flame frames. The proposed model with temporal slices was compared two similar DCGAN models but without temporal information and without the second training stage as well as to a CNN model with similar temporal slices. The results showed the DCGAN model with temporal slices achieved a high True Positive Rate of 92.19% and a low False Negative Rate of 3.91% which is better than the other compared models. The result indicates the robustness of the proposed GAN-based fire detection method and we highly recommended more works that investigate real-time application of such network for other flare analysis-related tasks such as smoke detection.

Another study by Xie et al. [11] implemented a Siamese network for detecting abnormal operation of flare pilot. The authors constructed a flare pilot anomaly detection dataset that contain picture of the flare in both normal and abnormal

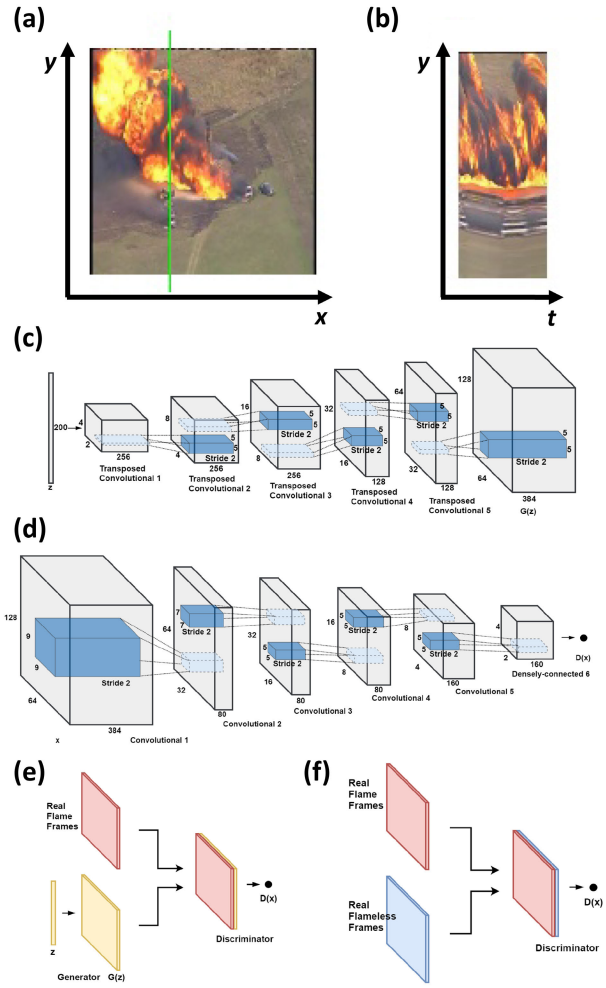

FIGURE 4. (a) A Flame smoke frame from the live video, (b) Presented temporal slice corresponding to the green line in Fig. (a), and structures of (c) the generator network, and (d) the discriminator network, (e) First training stage, (f) Second training stage [30].

operation conditions. Next, a Siamese network with a triplet loss function was designed for the detection of abnormal working conditions. During the training process, triplets of data were chosen so that the anchor image is similar to both positive (same type) and negative (opposite type) images which further improves the results of training. The network estimates the similarity of the picture with both positive and negative images to decide which category does the sample fit in. The accuracy of this model was compared to several popular deep learning models. The proposed model surpassed all other models in terms of classification accuracy which shows the huge potential of siamese networks in classification and detection tasks.

A novel approach for fire detection using video analysis, is proposed by [31]. The proposed method employs a deep learning model based on Xception [32] and Conv-Long-Short Term Memory (CONV-LSTM) networks. The Xception model is used to extract features from the input

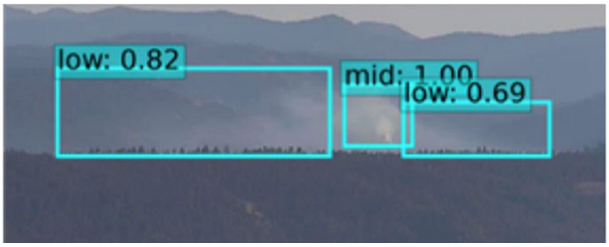

FIGURE 5. The sub-classification for the early-smoke recognition [44].

video frames, while the Conv-LSTM network is used to model the temporal dynamics (spatio-temporal information) of the video. The proposed model is trained on a large dataset of videos containing both fire and non-fire events. The results show that the proposed method achieves high accuracy in detecting fires in video sequences, where the classification accuracy of 95.83% has been reported. The authors also compare their approach with similar methods and demonstrate its superiority.

A recent study by Shahid and Hua [33] implemented a Vision Transformer (ViT) for the detection of fire in images. Vision Transformers have attracted huge attention from computer vision researchers recently as they can extract meaningful features spread throughout the spatial context [23].The authors used two sizes of the ViT network which are Base (Vit-B) and Large (ViT-L) and compared the obtained results from the ViT to those of other deep learning models, namely InceptionV1 [34] and SqueezeNet [35]. The models were tested using two popular fire detection data sets which were presented by Chino et al. [16] and Foggia et al. [20]. Comparison of the results showed that the ViT networks achieved higher classification performance compared to the other deep learning models. This work shows the huge potential of ViTs in fire detection and we recommend more works that use a similar method for smoke detection or real-time flare monitoring.

2) SMOKE DETECTION

The presence of smoke serves as an initial indication of fire, and its prompt identification has the potential to prevent the propagation of fire and minimize the associated risks to human life and material assets. However, the detection of smoke in natural surroundings presents an enormous challenge because of the diverse and fluctuating nature of smoke attributes, including its shape, color, transparency, motion, and texture [36]. Furthermore, the detection of smoke in outdoor environments is affected by a wide range of elements, such as but not limited to lighting conditions, weather conditions, camera resolution, and background clutter. Hence, it is imperative to develop robust and dependable techniques for the early detection of smoke using video processing.

There exist various approaches for detecting smoke, especially video-based smoke detection methods being commonly used [37]. These techniques can potentially be divided into

two primary categories: traditional techniques and deep learning techniques. Smoke detection in images or videos traditionally depends on manually designed features, including color, texture, motion, shape, and edge, to identify the presence of smoke. The aforementioned techniques frequently employ threshold, geometric segmentation, filtering, matching or clustering methodologies to extract relevant features. Subsequently, classifiers such as support vector machines (SVMs), KNN, and decision trees are utilized to differentiate between smoke and non-smoke regions. Nevertheless, it is important to acknowledge that these methods do possess certain limitations. For instance, they may be susceptible to noise, illumination variations, background interference, and occlusion. Additionally, they often necessitate manual parameter adjustments and exhibit a limited capacity for generalization. On the other hand, deep learning techniques employ neural networks to acquire knowledge about features and classifiers through the analysis of extensive datasets. These techniques possess the capability to autonomously extract high-level and abstract characteristics that exhibit enhanced resilience and distinctiveness for smoke detection. One typical realization of aforementioned methods are Convolutional Neural Networks (CNNs)-based structure, and Two-dimensional (2D) CNNs are predominantly employed for the purpose of detecting smoke in images, whereas Three-Dimensional (3D) CNNs are primarily utilized for smoke detection in videos [38], [39]. More recently, You Only Look Once (YOLO)-based [40], [41] structures are applied in this smoke detection field and YOLO now is at its 8th version [42]. Another subgroup for smoke detection is transformer-based structure such as Detection Transformer [43], [44], and temporal event transformers [45], [46]. In all, deep learning-based techniques can automatically extract features, eliminating the need for hand-engineered features. They excel at handling large and complex data sets, performing well across many tasks, and finding non-linear relationships in the data. These techniques can process images, text, and audio while requiring a lot of data and computation for training.

a: EARLY SMOKE DETECTION

Early smoke detection is a complex task which requires innovations that are both quick and precise to determine the presence of smoke in a variety of different environments. The nascent smoke is hard to be discovered both because of its light color, bad contrast with the background, and the distance [47]. Besides, since there is no benchmark (as different groups own different private data sets and can not build up each other), the instance number of existing early smoke data sets is limited [40], [48], [49], this fact makes the research even more difficult.

However, there are still some new signs of progress coming out from this field. For example Zhan et al. [50] applied a CNN-based Lightweight Model for seeking early-stage smoke from satellite images, they applied a Spatial Attention and Channel Attention combined method to achieve a regional and global attention combined attention structure so as to fully exploit the information inside the limited data set and achieved a final accuracy of more than 86%. In [51], Xiong et al. present a method to detect smoke in single-frame video sequences for forest fire prevention. The process has four steps: Firstly, the Simple Linear Iterative Clustering (SLIC) algorithm are applied to divide an image into small homogeneous regions for superpixel segmentation. Secondly, color similarity and edge information are used to merge superpixels, reducing over-segmentation and improving efficiency. Later, an improved algorithm is introduced to eliminate clouds and sky (which are often confused with smoke) so that the horizon line in one image can be identified. Finally, a Support Vector Machine (SVM) machine learning will classify those super-pixel blocks as smoke or non-smoke based on smoke spectral features. According to the paper, this method can eliminate noise like clouds and fog and detect smoke with 77% accuracy in a forest scene. Moreover, experimental results and comparisons with other methods are presented to demonstrate the method's efficacy and feasibility. This method may be used to monitor forest fires and provide early warning and automatic detection.

In 2022, Yazdi et al. [44] applied a structure that is based on the DEtection TRsformer (DETR) [43] while using a ResNet [52] as the backbone after the positional encoding. After defining special sub-classes for incipient-stage smoke, they achieved a successful classification for the early smoke even at a remote distance shown in Fig.5. Their obtained results illustrate the difficulty in recognizing and detecting search stages of smoke using only a single frame which highlights the importance of utilizing the temporal dynamics from multiple frames as an indicator for early-stage smoke evolution. Also in the same year, Masoom et al. [40] used a YOLO-PCA (Principle Component Analysis) method with an extra 4th scale specialized for the incipient-stage smoke and achieved a better-improved result than the traditional YOLO-V3 network in recognizing the smoke, however, no separate result for early-stage smoke detection was mentioned in this paper.

Kim and Muminov [39] adopted a methodology that utilizes YOLOv7 which is an advanced object detection model known for its ability to perform real-time image processing. In their paper, the YOLOv7 model is enhanced through the incorporation of a CBAM attention mechanism, an SPPF+ layer, and decoupled heads. These modifications aim to improve both the feature extraction and detection capabilities of the model. The employed approach additionally incorporates a BiFPN for the purpose of integrating multi-scale smoke features and acquiring learning weights to assign priority to the most significant feature maps. The approach assesses the performance of the model using a dataset comprising UAV images of forest fire smoke. Another approach employs the utilization of Xception, a deep convolutional neural network that employs depthwise separable convolutions to decrease parameter count and enhance computational

efficiency [53]. The proposed approach utilizes transfer learning by leveraging the Xception model, which has been pre-trained on the ImageNet dataset. Subsequently, the model is fine-tuned using a specialized dataset focused on fire and early smoke detection. The approach also incorporates the utilization of the learning without forgetting (LwF) technique, which is a method that maintains the initial capabilities of the model while acquiring knowledge related to a novel task. The approach evaluates the efficacy of incorporating learning without Forgetting (LwF) in the model across various datasets, demonstrating its ability to attain a notable level of accuracy and recall. In terms of early-stage smoke detection, another issue to be considered, again, is the required quick time response for the real-time video processing problem. Liu et al. [48] achieved this goal in an embedded platform by using a cascaded structure of AdaBoost classifiers together with some techniques such as Local Binary Pattern (LBP), histogram equalization, and image denoising (by Gaussian filter). They highlight that the smoke detection results can be derived by a lightweight device and achieve real-time monitoring of potential smoke. Those early-stage smoke will be sent back to the control center with a warning email and appended smoke frames from the video.

b: NORMAL SMOKE DETECTION

A study by Yin et al. [27] used a deep normalization and convolutional neural network (DNCNN) deep learning model for the detection of smoke in images. The DNCNN is a CNN that relies on sequences of normalization and convoutional layers for feature extraction followed by max-pooling and a fully-connected neural network classifier. The use of combined normalization and convolution layers helps in improving the detection performance and accelerating the training process. A database of smoke and non-smoke images was collected and used for training, validating, and testing the proposed model. The total number of images was 24217 and was divided as 10712 for training, 10617 for validation, and 2888 for testing. The obtained results showed excellent smoke detection performance with a detection rate of more than 96% and a low false alarm rate of less than 0.60%. The authors compared the performance of their model to those of other classical deep learning models which are VGG16 [54], ZF-Net [55], and Alex-Net [56]. It was found that the proposed DNCNN model showed superior detection performance compared to the other deep learning models while having a lower number of trainable parameters thus lowering the training time required. Finally, the authors compared their model to two other conventional smoke detection algorithms which are High-order Local Ternary Patterns based on Magnitudes of noise removed derivatives and values of Center pixels (HLTPMC) [57] and the Multichannel decoded Local Binary Patterns (MCLBP) [58]. The method achieved better performance compared to MCLBP and a comparable performance compared to HLTPMC as it showed a lower false alarm rate and a slightly lower detection rate. This work shows the potential of deep learning models for smoke detection compared to classical image processing and machine learning methods.

Another study by Gu et al. [59] proposed a dual-channel neural network (DCNN) deep learning model for the vision-based detection of smoke. The DCNN model consists of two subnetworks that work together and their outputs are concatenated to yield the model's detection output. The first subnetwork is a convolutional neural network (CNN) consisting of a sequence of convolutional layers and max-pooling layers with the addition of several batch normalization layers after some specific convolutional layers. The addition of batch normalization helps in mitigating the problem of overfitting and accelerates the training procedure. The second subnetwork is a CNN with components similar to the first sub network but with the addition of two extra components which are skip connections and global average pooling. The skip connection helps in reducing the effect of vanishing learning gradient and improves the propagation of image features while the global average pooling helps in overcoming the problem of overfitting and reduces the total number of parameters in the network. The first subnetwork was found to show good performance in extracting smoke features while the second subnetwork was better at capturing global information about the smoke present in the images. Concatenation of the outputs of the two networks helped in complementing the shortcomings of each of the subnetworks using the outputs of the second network. The DCNN model was trained and tested using the public smoke detection dataset published by Yin et al. [27]. The performance of the combined model was compared to that of eight state-of-the-art deep learning models which are Xception [32], Dense-Net [60], Res-Net [52], VGG-Net [54], Alex-Net [56]. ZF-Net [55], GoogLe-Net [61], and the deep normalization and convolutional neural network (DNCNN) [27]. The used model showed superior smoke detection performance with an accuracy of more than 99% which exceeds the accuracy values of the eight aforementioned models. Furthermore, the model was used to detect smoke released from a combustion flare in a petrochemical plant. The model was able to correctly classify nine images of flares as being ''with smoke'' or ''smokeless''; However, the amount of images that were used are too small to give an accurate performance estimation and no quantitative performance measure was mentioned regarding this application.

Later in 2020, Gu et al [62] proposed another novel image processing-based technique for the detection of flare soot in images named vision-based monitoring of flare soot (VMFS). The proposed method consists of three main steps. The first step focuses on detecting the flare's location as it is the main source of soot in the image. This is done using a broadly-tuned color channel based on modifying the red and blue channels that detect the color of the flare efficiently. If a flare is not located at this step, the algorithm terminates and the operation is labeled as not flaring and not sooting. In the next step, the location of the flare is extracted so that the

TABLE 3. Progress on visual segmentation of various flare-related objects. ('A': Accuracy, 'R': Recall, 'P': Precision, 'FAR': False Alarm Rate, 'TPR': True Positive Rate, 'TNR': True Negative Rate, 'mIoU': mean Intersection over Union. 'mMSE': mean Mean Squared Error).

Objective	Analysis method	Technique	Dataset	A	R	P	FAR	DR	FI	TPR	TNR	FPS	Year	Ref
Flame detection	Image processing	Color and Wavelet Analysis	VisiFire [14] Visor [15]					92.00					2017	[72]
		Multi-feature analysis	Own	97.02									2017	[74]
		Block-based eature analysis	Own				0.80	89.80					2020	[75]
	Machine learning	Texture analysis, extreme learning machine	VisiFire [14]					95.65		94.97		2.08	2018	[76]
		Color analysis, Gaussian Mixture Model	VisiFire [14]					94.40					2017	[77]
		Feature fusion, SVM	VisiFire [14]	74.20						98.37			2020	[78]
	Deep learning	CNN	Own							95.10		30.00	2018	[79]
		CNN	BoWFire [16] Foggia [20]	94.43	93.00	80.00			86.00	99.95	98.50		2018	[80]
		CNN, color conversion	Own	97.50	96.00	98.90			97.40			2.63	2021	[81]
		Two-stream CNN	Own	97.00						94.00	98.00		2019	[82]
		GAN	Own							92.19	96.09		2019	[30]
		Vision transformer	BoWFire [16] Foggia [20]	94.03	97.09	99.10			98.08	97.85	98.98		2021	[33]
Smoke detection	Image processing	Shape and color features	VisiFire [14] Yuan [17]	85.39	92.04	96.15			91.95				2017	[83]
		Saliency detection	VisiFire [14]						83.47				2020	[84]
		Color and Wavelet Analysis	VisFire [14] Visor [15]					87.00					2017	[72]
	Machine learning	HLTPMC , SVM	Yuan [17]					1.33	94.00				2016	[57]
		Flow-pattern analysis, temporal features, SVM	VisiFire [14] Visor [15]	97.40									2017	[73]
		Local and global feature extraction, SVM	VisiFire [14] CVPR-Lab-Fire [24] Foggia [20]				3.53			92.02			2018	[85]
		Sparse coefficients features, SVM	Own	94.90									2017	[86]
		Local binary pattern , Gaussian Process Regression	Yuan [17]				4.56	97.20					2017	[87]
		Robust AdaBoost	VisiFire [14] Visor [15]	91.25			0.31	99.69					2018	[88]
	Deep learning	CNN	Khan [19] Foggia [20]	94.76	95.00	98.00	2.06		96.00			39.84	2019	[18]
		CNN	Own	96.70			3.50	97.00				196.00	2018	[89]
		CNN (EfficientNet)	Khan [19] VisiFire [14] Yuan [17]	98.18	98.00	99.00	1.98		98.00			32.57	2021	[29]
		CNN with normalization	Yin [27]	97.96			0.48	95.82					2017	[27]
		Dual-channel CNN	Yin [27]	99.50			0.18	99.20				2.21	2019	[59]
		Ensemble deep CNN	Yin [27]	97.15	96.30	99.87			98.05		99.62		2021	[90]
		NN, transfer learmng	Own		98.98	98.49			99.30				2021	[91]
		CNN, Domain adaptation	Xu [28]					91.10					2017	[28]
		CNN, Motion detection	VisiFire [14] CVPR-Lab-Fire [24] Yuan [17]	99.06			1.04	99.25					2018	[70]
		Faster R-CNN	Own					82.10					2018	[92]
		Faster R-CNN and 3D CNN	VisiFire [14] CVPR-Lab-Fire [24]	91.88		93.18	3.77	84.72					2019	[71]
		Bidirectional LSTM	Own	97.80						97.50	8.00	10.37	2019	[96]
		Deep Belief Network	Own	95.00									2018	[94]
		Deep Belief Network	VisiFire [14]	93.00	100.00	92.00			96.00				2020	[95]
		Deep saliency networ	Xu [28]	98.12					90.08				2019	[96]
		Conv-RNN	CVPR-Lab-F1re [24]							95.25	98.53		2019	[97]
Soot detection	Image processing	Image color analysis	Own	99.76	100.00	99.33	0.02					2.28	2020	[62]
Soot density recognition	Deep learning	Meta-learning	Own	75.50			15.60	66.00					2020	[127]
Flare anomaly detection	Deep learning	Siamese networ	Own	99.00	98.00	100.00			99.00				2020	[11]

search for soot can be focused at that region. This is done using saliency detection which detects the most important objects in the image from a human inspector's point of view. Various saliency detection algorithms were tested and the one proposed by Hou et al. [63] named ''Image Signature'' was chosen as it showed the best performance. The saliency detection algorithm and the broadly-tuned color channel are combined with K-means clustering algorithm to remove the effect of any outlier detections. Finally, the last step uses a sequence of image processing operations to detect the pixels that contain the flare, correct for the color of the sky background, and search around the flare location for pixels that contain flare soot. If the total area of pixels that are labeled as ''soot'' pixels is more than zero then a conclusion of sooting operation is obtained; otherwise, the flare is operation in sootless mode. The proposed method was tested on four data sets of flare images in different operation modes and the performance was compared to several state-of-the-art deep neural network models, including Xception [32], DenseNet [60], GoogLe-Net [61], Res-Net [52], VGG-Net [54], Mobile-Net [64], the dual-channel deep network (DCNN) for smoke detection [59], and the deep normalization and convolutional neural network (DNCNN) [27]. The proposed model achieved more accurate classification compared to all eight before-mentioned models. The model also showed a very reliable detection performance as it achieved accuracy values higher than 99% on all four data sets while the other models showed a noticeable fluctuation in their performance. Furthermore, the proposed model showed the best execution efficiency as it required an average of 0.438 seconds per image which is the lowest among the other considered models. In order to improve the applicability of this detection approach we recommend investigating lowering the execution time of this method so that it can be applied in real-time monitoring systems.

3) ONGOING RESEARCH AND CASE STUDIES

In previous sections on flare and soot detection, the challenges in AI-enhanced remote inspection are acknowledged. To enhance the practical relevance of the article, the author includes this section of case studies to introduce how inspiring ongoing research in other areas can possibly benefit AI-enhanced Gas Flares detection.

As discussed, flare or smoke instances can be transparent and are easily mixed with a background like flog, cloud, or glare, these natures compromise the effectiveness

TABLE 4. Progress on visual segmentation of various flare-related objects. ('A': Accuracy, 'R': Recall, 'P': Precision, 'FAR': False Alarm Rate, 'TPR': True Positive Rate, 'TNR': True Negative Rate, 'mIoU': mean Intersection over Union 'mMSE': mean Mean Souared Error).

Objective	Analysis method	Technique	Dataset	A	R	P	FAR	Fl	TPR	TNR	mIoU	FPS	mMSE	Year	Ref
Flame segmentation	Image processing	Probablilistic color mappping	BoWFire [16]	90.07		93.67		87.23	86.02	93.70				2016	[110]
	Machine learning	Bayesian segmentation, SVM	Own					69.00						2015	[111]
	Deep learning	CNN	Own	98.10	89.00	79.40					72.30			2021	[107]
		CNN	FiSmo [25]	99.19	95.05	79.82	0.66	84.91			79.14	86.87		2021	[98]
			Corsican Fire [21]	97.46	95.17	94.46	1.87	94.70			90.02				
		CNN (DeepLabV3)	BoWFire [16]	97.79		73.27		79.14	87.42	99.45				2020	[26]
			Mlich [26]	99.00		82.00		85.00	88.00	99.20	70.51				
	Metaheuristic	PSO With K-Medoids clustering	Own	93.40					86.24					2017	[112]
Smoke segmentation	Image processing	Rough set theory	Own		100.00	92.00								2015	[113]
		LBP Silhouettes coefficient variant (LBPSCV)	Own						83.40	94.20				2020	[114]
		Saliency detection	VisiFire [14]		0.83	93.00								2016	[115]
	Deep learning	CNN	Own	92.50	90.70	94.10					85.80			2021	[107]
		CNN (DeepLabV3+)	Khan [19] VisiFire [14] Yuan [17]	93.33				50.76			77.86			2021	[29]
		Fully Convolutional Networks (FCN)	Own								69.81			2019	[111]
		3D Parallel Fully Convolutional Networks	VisiFire [14] Yuan [17]						87.07	89.31	79.75			2018	[116]
		Weakly supervised fine segmentation, lightweight Faster R-CNN	Own			99.60					70.20			2021	[117]
		Wave-shaped neural network (W-Net)	Own								73.97		0.02	2019	[118]
		Conditional GANs	VisiFire [14]		76.00	96.00						6.67		2019	[49]
		3D convolution-based encoder—decoder network	Li [116]						75.32	95.86	79.78			2020	[119]
		Classification-assisted Gate Recurrent Network (CGRNet)	Yuan [17]								81.67		0.23	2021	[120]

of current approaches in recognizing flare or smoke. To solve this difficulty, one possible solution is to use language prompts [22], [65]. These kinds of prompts, either in a fixed pattern or learnable format, can give the model extra hints about what the ROI (Region of Interest) contains. Besides, they can also improve the model's performance by using Image-to-Text Contrastive learning which can calculate the similarity between the extracted image feature and text feature and consequently deepen the model's understanding of complex tasks. Another potential solution mentioned is named 'anomaly detection' [66], [67]. Briefly speaking, a smoke or flare event can be regarded as a kind of abnormality, which is different from a normal event (nothing happened) in terms of behavior patterns, and object features. By quantifying patterns of normal events, abnormal events can be found to have a higher anomaly score or stronger association discrepancy [68] which can indicate the advent of a smoke or flare event. One more solution for detecting interested Gas Flares targets is to do temporal detection [69]. For the Gas Flares Inspection case. The existence of flare or soot has a continuous nature, which means there must be an event evolution before they can be obviously observed. Therefore, it is possible to embed existing models (like YOLO) with a temporal detection module so that this powerful YOLO module can be more specialized for Gas Flares tasks. This solution can be feasible because originally, YOLO could only perform single-image detection (which is called intra-image detection), by developing this Flare-soot temporal detection model, the YOLO may perform an inter-image detection so that the hint of flare or soot's existence can be easier observed.

In all, the aforementioned studies that successfully apply AI-enhanced visual inspection techniques in real-world scenarios could not only illustrate the potential of these ongoing technologies but also inspire further research to adopt them in the realm of Gas Flares detection.

4) SUMMARY AND DISCUSSION

There have been several works that discussed the detection of flare-related objects in images and videos. Table 3 summarizes the progress made on visual detection algorithms and their performances.

As can be seen in the table, various techniques ranging from image processing, machine learning, and deep learning were employed for the detection of flare-related objects. Most importantly, deep learning-based techniques were used the most for both flame and smoke detection tasks. This huge research interest is understandable in the shade of the many potentials that these techniques show in all computer vision-related tasks. The most used performance measures are the *Accuracy* (A) and the *Detection Rate* (DR) and high accuracy values of more than 99% were achieved by some techniques [59], [70]. However, a significant problem in these studies is the lack of common evaluation measures and unified benchmarking datasets. For example, Luo et al. [70] and Gu et al. [59] both achieved high detection accuracies but they tested their methods on two different datasets, making meaningful comparisons inapproachable. Moreover, studies that used the same dataset, for example the VisiFire dataset [14], mostly combined it with other datsets, such as in the case of Lin et al. [71] and Ye et al. [72] which combined that dataset with the CVPR-Fire-Lab dataset and the Visor dataset, respectively. Also, even when two works use the same datasets or the same combination of datasets, they mostly tend to use different performance measures such as Appana et al. [73] and Ye et al. [72] that used the same datasets but the first only reported the Accuracy and the second only mentioned the Detection Rate. These problems are of extreme importance in flame and smoke detection research and must be addressed by proposing unified benchmarking datasets and common evaluation measures that all future works adhere to.

B. SEGMENTATION

In the above section of detection, related references in the last 13 years have been concluded [14], [18], [27], [28], [29], [30], [33], [57], [59], [62], [70], [71], [72], [73], [74], [75], [76], [77], [78], [79], [80], [81], [82], [83], [84], [85], [86], [87], [88], [89], [90], [91], [92], [93], [94], [95], [96], [97]. In this subsection, the progress done on the segmentation of combustion-related object, namely flame and smoke, in gas flares scenes is summarized.

1) FLAME SEGMENTATION

There have been several works that discussed the visual segmentation of flame from RGB video stream. A study by Mlích et al. [26] implemented a state-of-the-art semantic segmentation deep learning model named DeepLabV3 for the segmentation of flame in images. Tested on the BoWFire dataset [16], the proposed model a high segmentation accuracy of 97.79% which was higher than other methods used in the literature. Next, the authors built their own segmentation dataset from publicly available flame images and tested the proposed model on it. The model achieved a high accuracy value of 99% and an excellent Intersection over Union (IoU) value of 70.51% on the proposed dataset. Their proposed dataset is available online and is a promising option for benchmarking flame segmentation models.

Another study by Choi et al. [98] proposed a novel deep learning-based flame segmentation technique using an improved version of the FusionNet deep learning network. The improved model employs input and output convolutional layers combined with middle skip connections for achieving improved feature feedback and enhanced segmentation accuracy. The proposed model was tested on two datasets which are the FiSmo dataset [25] and the Corsican Fire Database [21] and showed superior segmentation performance as it achieved segmentation accuracies of 99.19% and 97.46% on the two datasets, respectively. Moreover, the proposed model improvements was proven beneficial for the model's segmentation performance as the proposed model showed high IoU values compared to the normal FusionNet model and the same proposed model without the middle skip connections. This technique is of great potential and evaluating its performance in real-time monitoring systems is recommended.

A recent study by Bochkov et al. [99] proposed a novel deep learning model named wUUNet for multiclass flame segmentation. The new model is based on the UNet deep learning model and was improved for the flame segmentation problem. Multiclass segmentation was considered as different regions of the flame have different temperatures and recognizing the hottest regions in the flame is a crucial task in flame monitoring. The improved model includes skip connections between the decoder of the binary part and the encoder of the multiclass part of the model. The model was adjust even more by including the maximum number of possible skip connections between the binary part and the multiclass part of the model. The authors built a custom dataset of flame images and used it for evaluating the model. The model achieved a high mean segmentation accuracy of 95.34% and a low segmentation accuracy variance of 3.99. Finally, the model was shown to operate in real-time as it achieved an average segmentation speed of 63 frames per second. This model is of great potential for application in robotic real-time monitoring systems as it combines excellent flame segmentation performance with fast operation.

2) SMOKE SEGMENTATION

Smoke segmentation is an important task in the analysis of any combustion-related application. A recent study by Khan et al. [29] proposed a deep learning model based on Convolutional Neural Networks (CNNs) named "DeepSmoke" for detecting and segmenting smoke in both clear and foggy conditions. The authors fine-tuned a state-of-the-art deep learning network named Efficient-Net [100] for the smoke classification task and implemented a recent segmentation deep learning model named DeepLabv3+ [101] for smoke pixel-wise segmentation. The proposed system showed excellent detection performance as it achieved a high accuracy of more than 98% and a lower false alarm rate than other deep learning models, namely VGG-Net [54], Alex-Net [56], GoogLe-Net [61], and Mobile-Net-V2 [102]. Moreover, the system showed exceptional segmentation performance as it outperformed several state-of-the-art segmentation algorithms, namely Deconv-Net [103], FCN [104], DeepLab [105], and Seg-Net [106], by achieving higher mean Intersection over Union (IoU) and global accuracy scores in the smoke segmentation problem. The system also illustrated fast detection operation as it required an average execution time of less than 40 ms per frame which is equal to 25 frames per second. By looking at the accurate and fast operation of the system we highly recommend trying the implementation of this model in real-time monitoring systems such as drone inspection devices or stationary continuous monitoring systems.

Another study by Frizzi et al. [107] proposed a novel CNN-based model for detection and segmentation of smoke and fire from RGB images. The proposed segmentation method consists of two main stages which are the coding stage and the decoding stage. The first stage uses the architecture of the VGG16 network [54] and helps in extracting the local information of smoke and fire and its deeper layers enhance the generalization ability of the model. The second stage uses the information extracted through the first stage and generates a precise fire and smoke segmentation masks. During the second stage, feature maps from both stages are concatenated to give the model a deeper propagation of the fire and smoke contextual information. A data base of fire images was collected and labeled for the segmentation task. The performance of the proposed model was compared to two state-of-the-art segmentation networks which were proposed by Yuan et al. [108] and Ronneberger et al. (U-net) [109]. The

proposed model achieved better segmentation performance compared to the two other models for both smoke class and background class while have a slightly better performance to the work of Yuan et al. [108] regarding the fire class. The performance of the model in the fire class could be enhanced by increasing the size of the dataset and adding more pictures with fire.

3) SUMMARY AND DISCUSSION

As summarized from references [16], [17], [19], [21], [25], [26], [49], [107], [108], [110], [111], [112], [113], [114], [115], [116], [117], [118], [119], and [120]. There are multiple works in literature that discussed the segmentation of flame and smoke pixels in RGB images. Table 4 summarizes the works done on visual segmentation of flame and smoke and their performance measures. As shown in the table, different segmentation techniques including deep learning methods and image processing methods were used to segment flame and smoke images. Most-importantly, deep learning-based segmentation methods were used the most for both flame and smoke segmentation tasks. This is understandable as deep learning-based segmentation models have shown excellent performance in all types of segmentation tasks [121], [122]. Performance measures that were mostly used are the mean Intersection over Union (mIoU) and Precision (P) and high mIoU values of more than 85% were achieved in literature [98], [107]. However, similar to the case of flame-related object detection, the works in literature do not use the same image dataset for benchmarking which makes performance comparison inaccessible.

C. MEASUREMENT

Inspection using RGB cameras can be used for estimating important flare operation measures [123]. Minglu et al [124] introduced a new method for reconstructing the 3-D soot temperature and volume fraction of an afterburner flame using deep learning algorithms. The proposed method uses a two-camera setup to capture flame images from multiple angles, and then trains a convolutional neural network (CNN) to predict the soot temperature and volume fraction from these images. The authors compared the performances of their method, called StfNet-3D, with that of CNN, LSTM, and 3D TVR for reconstruction of 3-D soot temperature and volume fraction. The reconstruction accuracy, noise immunity and computational costs were used to verify the performance of each reconstruction algorithm. Overall, the paper's findings suggest that the proposed deep learning-based method has significant potential for improving the monitoring and control of afterburner flames in various industrial applications, including flare gaz invliving-industries.

A study by Johnson et al. [125] investigated the application of an image-based technique named sky-line-of-sight attenuation (sky-LOSA) for the estimation of soot release amount from an operating gas flare. The method relies on two cameras for visually inspecting the flare plume and estimating the soot emission rate along the plume axis, as shown in Fig. 6 (a). The first camera is a high-frame rate camera that is used to estimate the velocity of the emitted plume using the visual data collected at 300 frames per second. The second camera is a thermoelectrically-cooled CCD camera with a specific band-pass filter and is used for collecting monochromatic images of the plume. After data collection, the images were processed for estimating the soot emission rate as shown in Fig. 6 (b-g). The images were rotated, corrected for the sky effect, and combined with the average velocity data obtained using the high-frame rate camera. Next, the value of the soot emission rate was estimated by summing horizontally over the combined image using the following equation:

$$\overline{\dot{m}_{soot}} = \frac{1}{N_f}\frac{1}{N_z}\sum_{j=1}^{N_z}\sum_{i=1}^{N_f} A \int U(y,z)_j ln(\tau_\lambda(y,z)_{i,j})dy \quad (3)$$

where N_f is the number of ensemble measurements, N_z is the number of measurements in the z-direction, $U(y, z)$ is the average velocity at the point (y, z), $\tau_\lambda(y, z)$ is the transmissivity at the point (y, z), and A is a constant term related to the soot characteristics and optical parameters. Using this method, the average soot emission rate along the plume's axis was successfully measured as shown in Fig. 6 (h). However, the uncertainty of this method was approximated to be around 33% which is too high to be considered reliable. Thus, further investigations of such measurement technique is highly recommended especially for reducing the uncertainty of the measurement.

Another study by Castineira et al. [126] discussed the application of Multivariate Image Analysis (MIA) using Principal Component Analysis (PCA) and projection to latent structures (PLS) for the analysis of combustion flares through the use of color RGB images. This technique estimates the flares combustion efficiency as a function of the wind speed and the air or steam flow rates by implementing a combination of simulations and experiments. This technique was applied successfully for finding the combustion efficiency using the RGB images in a specific range of operation conditions. Studies that implement a similar methodology but using deep learning regression techniques are highly recommended. Moreover, studies that follow the same technique but with the use of hyperspectral and multispectral images are recommended as including multiple spectra will provide more information to the prediction model and thus is expected to achieve higher prediction accuracy.

Gu et al. [127] proposed a deep learning model that combines model-agnostic meta-learning (MAML) algorithm combined with selective ensemble for the density prediction of flare soot using only few-shot data. As the problem of flare soot occurs rarely on very limited data are available for such condition, the use of few-shot learning is of extreme importance. In the beginning, MAML was used to provide general-purpose optimized initial parameters (GOIP) for the

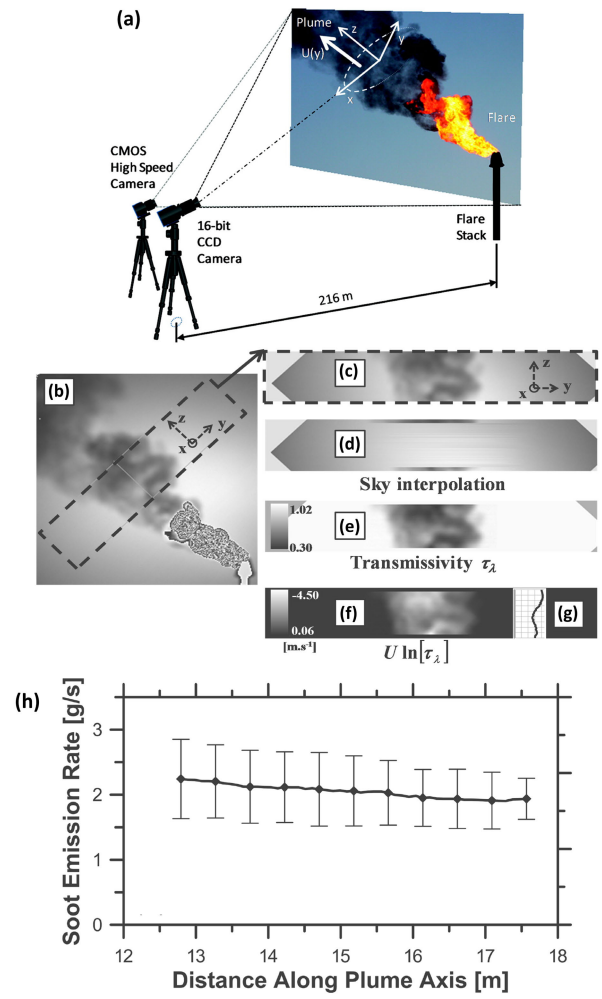

FIGURE 6. (a) The flare imaging setup used for the sky-LOSA technique, (b) An image obtained using the CCD camera, (c) A rotated section from the image, (d) The section with the interpolated sky intensity, (e) The transmissivity image (the ratio of picture (c) to picture (d)), (f) Combination of transmissivity image with ensemble-averaged velocity data, (g) Vertical profile of the combination, (h) The measured soot emission rate profile along the plume's axis [125].

soot analysis task by training models on very similar other tasks such as the detection of water vapor, cigarette smoke, and dark clouds. This steps gives the model a high generalization capability. After that, these initial parameters are used during the training procedure with a novel ensemble that is implemented to combine various predictions using a wide range of learning rates and a few gradient descent steps. The authors started the prediction task with vision-based monitoring of flare soot (VMFS) model [62] to check for the occurrence of flare soot. Next, the proposed model by the authors was used to give a prediction in a binary classification task where the output is either light soot of dense soot. The results of the proposed model were compared to several state-of-the-art deep learning models, including Xception [32], Dense-Net [60], Res-Net [52], VGG-Net [54], Alex-Net [56]. ZF-Net [55], GoogLe-Net [61], and the dual-channel deep network (DCNN) for smoke detection [59]. The proposed model showed better performance compared to the other models in the task of soot density recognition as it achieved a higher average accuracy ratio, a higher average detection rate, and a lower average false-alarm rate when the testing process was done five times. However, the obtained results showed a relatively high standard deviation in the accuracy values, which shows the need for further improvements to this model to increase its reliability.

IV. HYPERSPECTRAL IMAGING FOR COMBUSTION FLARE ANALYSIS

In the last year, hyperspectral imaging have attracted huge attention from many researchers as a promising tool for various optical inspection and analysis applications. It was applied in various fields such as food industry [128], [129], [130], agriculture [131], [132], environmental monitoring [133], medical applications [134], [135], [136], and materials engineering [137]. Hyperspectral images provide richer information about the captured scene as they provide continuous spectral information compared to the three specific channels in RGB images. Every pixel in a hyperspectral image is a profile of hundreds of reflectance values corresponding to many narrow-band spectral channels. These profiles can be used to derive many useful information about the pixel such as the involved compounds, the compounds ratios, the temperature profile, and the emitted radiative power. Recent hyperspectral imaging systems provide enough spectral resolution for deep analysis of the scene while ensuring enough spatial resolution for covering the entire desired scene and data acquisition speed for rapidly changing scenarios [138]. In this section, the application of various hyperspectral imaging systems, such as infrared sensors and spaceborne hyperspectral remote sensing systems, is reviewed and discussed.

A. DIRECT FLARE PERFORMANCE ESTIMATION

One of the most common methods in analyzing combustion flares is by using a stationary infrared imaging system that is mounted a distance away from the flare. These infrared sensors are directed toward the flare or toward its exhaust gas and are used to evaluate the flare's combustion performance by measuring the ratios of the chemical products in the exhaust gas. The composition ratios can be used to measure the flare's combustion efficiency and other related flare performance measures. The most common infrared sensors for flare inspection are Fourier-transform infrared spectroscopy (FTIR) sensors which can extract useful information about the flare system via obtaining infrared absorption/emission spectra. In this subsection, the progress done on direct gas flares performance estimation using hyperspectral sensors is reviewed.

1) COMBUSTION EFFICIENCY ESTIMATION

A study by Blackwood et al. [139] applied an open-path FTIR (OP FTIR) imaging system to estimate the combustion

efficiency of an industrial flare. The imaging system was implemented to be compared to several combustion models. The imaging system was applied to low-btu flares which are commonly known for low combustion efficiency values of around 30% according to many combustion models. However, when the author used the OP-FTIR imaging system to estimate the combustion efficiency, values of more than 90% were achieved. The methods that were used to estimate the combustion efficiency were monitoring the CO to CO_2 ratio, monitoring CO to tracer gas ratio (SF_6 and CF_4), and the application of dispersion models. The experimental results obtained illustrate that theoretical models such as the model developed by Leahey et al. [140] need to be improved in order to agree with experimental data.

In the work of Wormhoudt et al. [141] a comparison between a remote sensing technique based on passive FTIR (PFTIR) and an extractive sampling method for combustion flare analysis was carried out. The goal of the study was to estimate the flare combustion efficiency and to compare the two flare analysis techniques in terms of the estimation accuracy. The authors found that both techniques were able to accurately determine the combustion efficiency and the flare performance curves. However, in the cases where a noticeable difference was found between the two measurement techniques, the main reason was the inaccuracy in estimation of the main component of the fuel by the PFTIR sensor. Thus, improving the measurement accuracy of the elements in the exhaust is required for the PFTIR technique to be applied in other more complicated applications involving combustion. The obtained results showed that the problem of inhomogenety in the flare exhaust did not affect the measured combustion efficiency values in a significant matter.

A similar work by Gagnon et al. [142] discussed the application of a thermal hyperspectral camera based on FTIR spectroscopy for industrial smokestack and flare analysis. The authors used a commercial Hyperspectral imaging system named ''Telops Hyper-Cam Very-Long-Wave'' which can be used to study the chemical composition and the spatial distribution of the analyzed flares from large distances. First, the instrument was used to study the composition of a smokestack and a flare from a distance of more than 1 kilometer. The authors were able to examine the chemical components of the smokestack and the flare by comparing the obtained FTIR profiles to reference elements profiles. Next, the authors used the obtained hyperspectral data to examine the spatial distribution of the chemicals in the smokestack. They were able to predict the regions with relatively higher chemicals content in the obtained images. Finally, the obtained data were used to estimate the combustion efficiency of the flare by comparing the temperature profile with the oxygen and gas profiles. This imaging systems shows great potential for chemical analysis of combustion flares and smokestacks and we recommend doing more comparative studies with extractive sampling data.

Similarly, Huot et al. [143] discussed the application of a hyperspectral imaging system for the analysis of a combustion reaction. The authors used a hyperspectral camera named ''Telops MS-IR MW'' for high frame-rate imaging combined with a motorized filter wheel of 8 filters to allow for time-resolved imaging of the combustion products. The imaging system was applied to analyze a candle with the combustion and burst of black powder. The temperature of the combustion was estimated using the obtained hyperspectral images from the 8 filters and was compared to other conventional broadband imaging techniques. Spatial and temporal information of the temperature during the burst were obtained using the hyperspectral imaging system and the results agreed well with other methods that were used previously.

Another work by Zeng et al. [12] studied the application of a novel remote method for the analysis of combustion flares which is based on hyperspectral infrared imaging. The used imager was first proposed by Zeng et al. [144]. This imager has the advantages of high image resolution, high spectral selectivity, high imaging frame rate, and the suitability for short-term analyses and long-term continuous monitoring. The proposed method was implemented to measure the combustion efficiency of the flare and to estimate the amount of smoke formed regardless of the lighting condition. Estimating the amount of smoke helps the operator in optimizing the flare's performance by reaching the ''incipient smoke point''. The accuracy of the novel method was validated by comparison to an extractive sampling monitoring system in batch-scale experiments. The obtained results indicated high accuracy for the infrared imaging-based method as it showed great agreement with the extractive sampling results indicated by an R^2 value of 0.9856 and an average deviation of around 0.5%. The accuracy of the used methods was better in the cases of higher combustion efficiency as the method slightly overestimated the values at lower combustion efficiency situations. However, this is still acceptable as flares do not typically operate at such low combustion efficiency values. Next, the amount of smoke produced from the flare was measured using the ''smoke index'' which is a unitless number that increases as the level of smoke generated increases. This unitless metric was evaluated successfully to estimate the amount of smoke in different scenarios. The proposed system is very promising in both short-term and continuous monitoring applications and we highly recommend doing more experimental studies for the same technique in different flare situations.

2) TEMPERATURE PROFILE ESTIMATION

Another study by Moore et al. [145] discussed the application of FTIR-based hyperspectral camera named ''Telops Hyper-Cam MWE-Fast'' for the analysis of turbojet exhaust. Due to the highly changing nature of turbulent turbojet exhausts, scene-change artifacts were present in the observed spectra by the hyperspectral camera. These artifacts result in high frequency noise. The authors used moderate temporal averaging to reduce the effect of this noise on the analysis results. The chemical composition of the turbojet exhaust that contains

CO and CO_2 was successfully analyzed and the temperatures and relative concentrations of each of these elements were obtained. The complicated nature of such flow fields required the development of more accurate combustion and fluid dynamics models to make analysis of such flows more accessible.

B. INDIRECT FLARE PERFORMANCE ESTIMATION

The obtained hyperspectral data can be used indirectly for obtaining useful information on the gas flare's performance. The methods that were used extensively in analyzing gas flares include the application of combustion models and theoretical analyses. These techniques allow for inspecting and analyzing systems when no direct methods can be used. In this subsection, the progress done on indirect gas flares performance estimation using hyperspectral sensors is summarized.

1) HYPERSPECTRAL DATA MODELING

There are several works that discussed the modeling of hyperspectral data for gas flare monitoring. A study by Panfili [3] proposed a high-fidelity forward model for the use in processing hyperspectral imaging data and finding the combustion efficiency of flares. The model was proposed to be an element of a retrieval algorithm for extracting useful information from raw hyperspectral data. The main inputs of the model were the molecular concentrations and the layer temperatures and the model outputs the spectral radiance for each band and the Jacobian matrix of the parameters derivatives. This modeling approach was implemented in a software and compared to another applied model which is SHARC and MODTRAN Merged Code (SAMM) [146]. The results showed close but not identical predictions between the two algorithms due to the differences in the assumptions and the modeling procedure. This modeling approach is still incomplete and more works that build on this proposed model are required to be able to find the combustion efficiency of flares using hyperspectral data.

Another study by Grauer et al. [147] proposed a new model for the estimation of emission rate from a plume of heated gas. The methods relied on hyperspectral data obtained using FTIR spectroscopy measurements and the radiative transfer equation to derive a gaussian model for volume fraction and temperature. In order to test the proposed model, the authors estimated the emission rate of a simulated heated methane plume by using synthetic hyperspectral images. By comparing the gaussian distributions-based model to uniform distributions model, the gaussian model achieved higher accuracy in column density estimation by 14%. Moreover, the emission rate estimated by the gaussian model was within 4% true value. It is recommended that the same approach be applied for the estimation of other flare parameters such as the flare combustion efficiency.

One of the important uses of modeling in hyperspectral imaging is for providing a reference spectrum for comparison with the experimentally obtained spectrum. A study by Taylor et al. [148] discussed the use of hyperspectral imaging based on FTIR technology for the detection of highly-reactive volatile organic compounds that form ozone and dangerous human carcinogens. In order to provide reference for the obtained FTIR images, the methods relied on spectroscopic databases when they are available and on quantum chemistry computation whenever spectroscopic data were not available. The authors compared their analytical results to experimental results obtained from the Pacific Northwest National Laboratory Infrared Spectral Library (PNNL IRSL) for some organic molecules, namely formaldehyde and 2-butene. The results showed good agreement for the smaller molecule which is formaldehyde (Fig. 7(a)) and more deviation for the bigger molecule which is 2-butene (Fig. 7(b)). The differences between the two profiles indicate that more improvements in the theoretical model are required. This method can be a potential solution for detection of organic compounds with low data availability. Another similar work by Panfili et al. [149] used an identical approach to find the spectra of large organic molecules with no data available. The authors used an analytical model to find the spectra of Ethyl-Benzene, Toluene, and Ortho-xylene. They achieved similar results where larger molecules result in less accurate modeling and thus an improved approach is required.

Another study by Han et al. [150] discussed spectrum modeling and the effect of different environmental factors on the released spectrum of a combustion flare in the mid-wave infrared region. The authors used a line-by-line modeling strategy to model infrared spectra and increased the accuracy of the modeled spectra by taking spectral line broadening into consideration. Preliminary infrared spectra were obtained using the high-temperature molecular spectroscopic database (HITEMP) and collisional broadening at pressures higher than 0.1 atm was considered as it is the most dominant spectral line broadening phenomenon. The main products of the flare that was considered for modeling were CO_2, H_2O, CO, and N_2. However, N_2 was ignored in the analysis as it did not interfere with the spectra in the infrared range. Also, the temperature of the considered flare was assumed to be 2000K. First, the effect of the instrument function on the observed spectra was discussed. It was found that lower spectral resolution of the instrument results in lower observed spectra especially in wavelengths where more fluctuations are present. Next, the effect of various parameters that are related to the radiation transmission in the atmosphere, namely the horizontal distance, the vertical distance, the measurement angle, and the humidity. It was found that increasing both horizontal and vertical distances, lowering the measurement angle, and increasing the humidity resulted in lowering the observed spectra. However, it was noticed that the effect of the horizontal distance was much more significant compared to the vertical distance as the density of air molecules in high vertical distances decreases gradually and thus results in lower spectral losses. Finally, the obtained results were compared to experimental results for validation

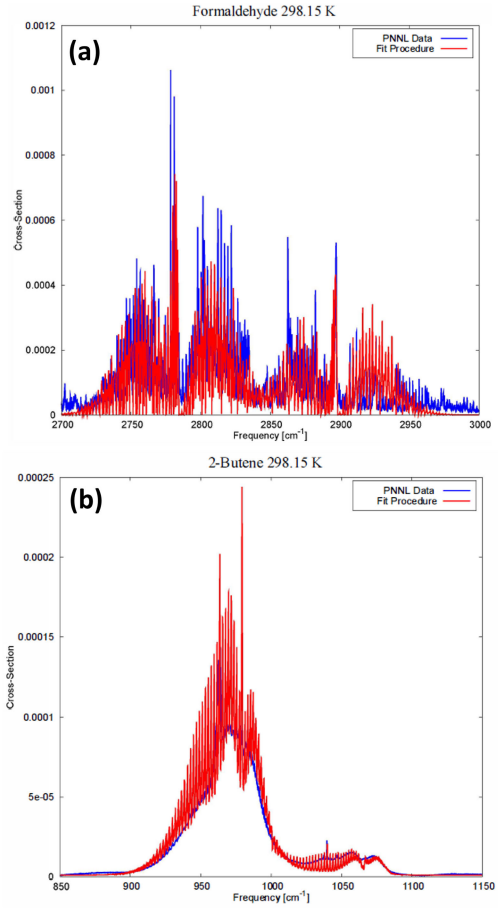

FIGURE 7. Comparison between experimental (blue) and analytical (red) spectra for (a) formaldehyde and (b) 2-butene at 298.15K [148].

the two data showed excellent agreement with a root-mean-squared (RMS) deviation of about 6.7%. We recommend doing similar studies on different types of flares with different reaction products such as H_2S and in different operational conditions as this will fit with a wider variety of combustion-based applications.

2) THEORETICAL ASPECTS OF HYPERSPECTRAL FLARE MONITORING

There are other works that discussed different theoretical aspects of hyperspectral flare monitoring. A study by Conard et al. [151] discussed the effect of beam steering on remote measurements of combustion flares and emissions. Beam steering occurs when light deflects as it goes through gases with different compositions. The phenomenon reaches its extreme case when light goes through heated gases with significantly different composition, which is the case for combustion flares emissions. In order to assess the effect of beam steering on the analysis of combustion flares, the authors derived three multiplicative correction parameters for the effect of beam steering on source intensity, incident intensity, and optical depth. The results showed that even at the most extreme cases, the correction parameters only deviated very slightly from unity, and taking into consideration the instrument error and noise, these three parameters can practically be taken as unity. This proves the problem of beam steering can be neglected safely when hyperspectral imaging of combustion flares is implemented.

Another study by Miguel et al. [152] proposed a method for selecting the optimal filters of an infrared hyperspectral imaging system that is used for analyzing combustion flares. The method proposed by the authors relied on ranking the filters based on the ratio of the quantity of interest's variance to the noise variance where better filters will have lower ratio values. The validity of this ranking criteria was checked by evaluating the combustion efficiencies using different filters and inspecting the accuracy of the obtained measures. It was found that filters with a lower ratio values achieved more accurate combustion efficiency estimates.

C. FLARING ACTIVITY ANALYSIS

There have been many studies that discussed the detection and analysis of flares using satellite-mounted remote sensing technologies. These technologies allow for monitoring the overall flaring activity in a region throughout time which is an essential task in environmental emission monitoring. There are two main types of spaceborne monitoring methods. The first is daytime sensing that uses day time hyperspectral sensors to locate and inspect flares. This technique is of limited capability as the background radiation is too high which makes detecting small flares harder. The second type is nighttime sensing that locates flaring activities during night. This technique is of much higher capability as it does not get affected by solar radiation reflected from the earth surface and thus can be easily used to detect and monitor smaller flares. These methods are used mainly for two tasks. The first is detection and localization where the total number of flaring activities is analyzed spatially and temporally. The second is parameter estimation where relevant performance parameters such as the flare's temperature, the flared gas volume, and the source's size are obtained. In this section, the progress done on various flaring activity analysis methods is reviewed.

1) DETECTION AND LOCALIZATION

An important task in the analysis of flaring activity is detecting and localizing the flares both spatially and temporally using hyperspectral sensors mounted on satellites. A study by Chowdhury et al. [153] discussed the use of multispectral images taken by the Landsat-8 satellite for daytime detection of industrial flares. A detection algorithm named Sequential Maximum Angle Convex Cone (SMACC) was employed to detect endmembers in the hyperspectral images and thus detect flares as bright pixels in the hyperspectral data. The method was applied to three locations in Alberta, Canada, and 31 flare locations were successfully detected. The authors verified the presence of flares by comparing the observed locations with satellite images of the Earth surface from

Google Maps and Microsoft Bing Maps. This method is promising for daytime flare detection as it is a more challenging problem compared to nighttime flare detection.

Another study by Casadio et al. [154] proposed a new strategy for detection of industrial flares from space using Along Track Scanning Radiometer (ATSR) measurements. The new strategy named ALGO3 relies on radiations in the Short-wave infrared (SWIR) wavelengths that was observed by satellites with ATSR family instruments. The detection scheme was based on the idea that industrial flares will have consistent radiations in the SWIR band throughout the year while natural fires will have much lower number of occurrences and the night-time background radiation in the SWIR range in negligible. This method has the advantages of only detecting currently active flames with temperatures exceeding 850K, working efficiently in all latitudes, and by the use of SWIR combined with Mid-Infrared (MIR) and Thermal-Infrared (TIR) the observed flares can be categorized in terms of the size and temperature. The authors validated the accuracy of their strategy by examining high resolution satellite images of the Earth surface and verifying the presence of industrial flares.

In another work, Schroeder et al. [155] proposed an algorithm for the detection of various fire scenarios using both daytime and nighttime hyperspectral satellite data. The data were collected using Landsat-8's Operational Land Imager (OLI) during both daytime and nighttime from several sites globally and were used for the detection of industrial gas flares, active volcanoes, and biomass burning. Daytime data are used to detect unmistakable fire locations and the nighttime data is used to identify smaller fires that are harder to detect using daytime data. The algorithm showed excellent performance in detecting active fires with large areas and improved performance for small-area fires. A low commission error value of around 0.2% was achieved for the data collected throughout the world.

Similarly, Elvidge et al. [156] discussed extending the detection capability of the VIIRS data-based NightFire algorithm by including infrared spectral data from the Day/Night Band (DNB). The inclusion of the DNB has the potential of significantly increasing the number of detected combustion flares by including flares with a much smaller area of 0.001 m^2 at a typical temperature of gas flaring of 1800K. The authors used DNB data alongside the conventional VIIRS bands to detect flare location in a specific region in India in 2015 and were able to detect a 15 times increased number of flares compared to the method that only uses the conventional bands. These results show the potential of a VIIRS-based detection algorithm that takes into account the DNB data to provide a more comprehensive detecting algorithm that will further increase the practicality of this technology.

2) PARAMETER ESTIMATION

After the flaring activities are located in the study region and period, the next task is analyzing the collected data for obtaining useful information about the individual flares and the total flaring trends. This is done by estimating various performance parameters of the flares using hyperspectral data. A study by Elvidge et al. [157] discussed the application of Visible Infrared Imaging Radiometer Suite (VIIRS) spaceborne sensors for detection and analysis of combustion flares during nighttime. The authors used nighttime infrared radiation date from the NIR and MWIR bands collected using the VIIRS sensor and the Nightfire algorithm to detect the locations of flares and to estimate several important performance measures. The algorithm relies on modeling the blackbody radiation curve using Planck equation and then compare both observed and modeled data to estimate the source's temperature (K), the fire radiative power (W/m^2), the total radiated heat (MW), and the source's size (m^2). The results showed that the use of nighttime data is much more suitable for usage with the proposed algorithm as the obtained data clearly indicate locations of flares. Furthermore, the algorithms was successfully used to estimate operational measures of several existing combustion flares and biomass combustion sites. The same method was used by Elvidge et al. [158] for estimating parameters of biomass combustion in Sumatra and the results showed excellent agreement with the data obtained by Moderate Resolution Imaging Spectrometer (MODIS) spaceborne detector.

In another study, Anejionu et al. [159] proposed two novel techniques for the detection of gas flares and estimation of total flared gas volumes using Moderate Resolution Imaging Spectroradiometer (MODIS) nighttime infrared satellite data. The two proposed techniques which are named the MODIS flare detection technique (MODET) and the MODIS flare volume estimation technique (MOVET) were implemented to study the flaring activity in Niger Delta, Nigeria between 2000 and 2014. Implementation of the two methods resulted in detailed temporal and spatial analysis of the flaring activity in the studied region. This method is of high potential as it allows for easy and fast analysis of flaring activities especially in regions where access to flaring data is limited or restricted.

Also, another study by Elvidge et al. [160] used hyperspectral data collected using the same VIIRS spaceborne sensor to estimate the total worldwide flares number and total emissions in 2012. The authors located 7467 flares worldwide using VIIRS data and specified the countries with the largest number of flares and the larges number of flared amount, as shown in Fig. 8. It was found that the USA had the largest number of operational flares in 2012 of 2399 flares while Russia had the largest amount of flared gas volume of 24.6 billion cubic meter (BCM). The authors also analyzed the detected flares using Planck equation to estimate the most important operation parameters. They showed that there are two main problems in the estimation of operation parameters using VIIRS which are the inaccurate estimates of weakly detected flares and unsuitability for monitoring flares with unsteady operation times. Finally, a correction for the view angle from the spaceborne sensor was proposed using

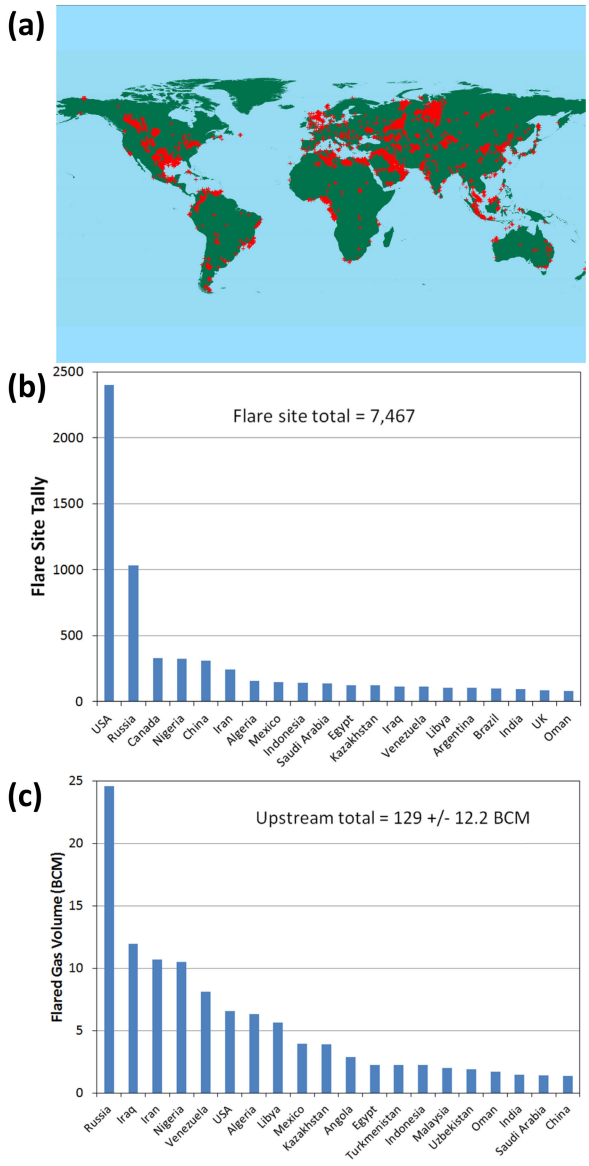

FIGURE 8. (a) Location of flares detected using VIIRS sensor in 2012, image is presented in a global scale, (b) Number of flares detected in each country and (c) Total amount of flared gas in billion cubic meter (BCM) in 2012 [160].

the ellipticity coefficient which resulted in more accurate measures. These works show the great potential of VIIRS in nighttime spaceborne flare monitoring and similar studies that apply the same methodologies using more recent data are highly recommended.

Another work by Faruolo et al. [161] developed a spaceborne inspection technique named Robust Satellite Techniques-FLARE (RST-FLARE) algorithm that uses nighttime Moderate Resolution Imaging Spectrometer (MODIS) sensor data for localization and parameter estimation of combustion flares. The authors used the proposed technique to study the flaring actions in the Niger Delta region, Nigeria, and monitor the change in flaring activity during the period from 2000 to 2016. The algorithm successfully estimated the number of flares and localized them throughout the 17 year study period and illustrated good agreement with results obtained using other spaceborne techniques (MODET, MOVET, VIIRS NightFire) and data from a national organization (Nigerian National Petroleum Corporation). A localization accuracy of 95% and an error mean in the emission volume estimates between 16% and 20% were achieved when the obtained results were compared to the before-mentioned baselines. As an extension to their previous work, Faruolo et al. [162] proposed a modification of the Robust Satellite Techniques-FLARE (RST-FLARE) algorithm to be used with the VIIRS hgperspectral data instead of MODIS data. The motivation for this modification was to benefit from the enhanced spectral and spatial properties of the VIIRS sensor and to ensure the continuity of spaceborne inspection after the possible end of MODIS sensor's life. The authors used the modified algorithm to monitor the emissions from the Val d'Agri Oil Center in Italy in the period from 2015 to 2019. The obtained results showed great agreement with the estimated of the VIIRS NightFire algorithm in terms of the radiant heat estimated from the combustion site. The excellent results obtained by this modified method suggest the development of a hybrid RST-FLARE algorithm that uses data from both MODIS and VIIRS sensors to obtain more accurate inspection results.

In another work, Fisher et al. [163] discussed the use of Short-wave infrared (SWIR) radiation data for the estimation of Fire Radiative Power (FRP) of industrial flares. The authors first tried using Mid-wave Infrared (MWIR) radiation data but these data were not suitable for FRP estimation of industrial gas flares as the operating temperature was too high for this methods to be used. SWIR data were used instead and much more accurate FRP estimates were achieved. When analyzing industrial gas flares in the temperature range between 1600K and 2200K, the proposed estimation method resulted in maximum errors within 13.6% and 6.3% at radiation wavelengths of 1.6 μm and 2.2 μm, respectively. Finally, the obtained results were compared to the estimates of multispectral Visible Infrared Imaging Radiometer Suite (VIIRS) NightFire algorithm and the two measures showed great agreement. This method is of great importance as it can be used to analyze industrial gas flares using old satellite sensors such as ATSR in the period from 1991 to 2012 that can not be directly analyzed using normal multispectral analysis algorithms.

A recent study by Franklin et al. [164] utilized VIIRS hyperspectral satellite data and the Nightfire algorithm to investigate the flaring activity in the Eagle Ford Shale region in Texas, US. The spaceborne data were collected in the interval from 2012 to 2016 and was used to locate the flares and estimate their total flared gas amount in the study period. The analysis located 43887 flares in the specified region and period and the total flared gas volume was estimated to be 4.5 billion cubic meters. Furthermore, the amount of gas flared from each flare was estimated using reported flare

emission data from the Railroad Commission of Texas and the obtained VIIRS satellite data. This application shows the ability of VIIRS data to provide both spatial and temporal analysis of various flaring activities. More recently, in 2023, Zhang et al. [165] also used the VIIRS sensor for wildfire detection in Southeastern Australia. In their case, random forest (RF) data processing techniques (with its 2 variants named RF-N and RF-D) are selected as investigation objects, while collected spatial-temporal matching information from different VIIRS sensors are regarded as ground-truth. After training and several trials in finding optimal hyper-parameters, they achieved good recognition results in association with both RF-N and RF-D models. Besides, the author evaluated these RF-based models via counting their feature importance and measuring the performance uncertainty which is followed by visual comparisons between their RF fire detection results and that of VIIRS sensors. Presented results illustrate that the trained RF models are highly capable in terms of detecting wildfire within large-scale satellite images.

D. SUMMARY AND DISCUSSION

There have been several works in the literature on the application of various hyperspectral imaging techniques for flare analysis. These works ranged from experimental on-site monitoring using infrared sensors and space-borne remote sensing using satellites to theoretical spectra modeling. Regarding direct flare inspection, the most used inspection technique is the FTIR sensor. This is due to its ability in accurate flare performance estimation and its commercial availability. For indirect flare analysis, various mathematical models were employed to obtain the hyperspectral spectrum in cases where it was not directly available. These methods are of great benefit, especially in the case of monitoring the flaring of uncommon compounds. Regarding flaring activity analysis, various satellite sensors were used for detecting, localizing, and performing measurements for gas flaring activities for specified regions and time periods.

V. MULTI-VIEW INSPECTION OF COMBUSTION FLARES

Multi-view inspection is one of the important techniques for achieving accurate and fast flame and smoke monitoring in various applications [10], [166], [167], [168]. The utilization of video streams from multiple cameras located in different locations allows for detecting flame and smoke faster and attaining a more accurate estimation of the current combustion state. A study by Verstockt et al. [169] illustrated a multi-view inspection framework named "FireCube" for detecting and localizing flame and smoke from a combustion source. This inspection techniques allows for fast flame and smoke detection in the early stages of combustion by merging the obtained views of multiple cameras using homographic projections onto several vertical and horizontal planes. By merging the obtained homographic projection planes, a 3D grid of virtual monitoring point is obtained. This 3D grid combined with 3D temporal and spatial filtering allows for obtaining accurate and reliable localization information of the flame, including its size and propagation direction. The proposed method was tested with only two cameras and the system achieved an excellent flame localization performance illustrated by a high dimension accuracy of 90% and a near-perfect position accuracy of 98%. The method also achieved an excellent detection accuracy of 90% when only two cameras were used. Moreover, the technique could achieve even higher performance by using more than two cameras as a dimension accuracy of 96%, a position accuracy of 99%, and a flame detection accuracy of 92% can be obtained when four cameras are used. Further increasing the number of monitoring cameras is expected to further boost the detection accuracy and dimension accuracy.

In a recent study, Cheng et al. [170] developed a multi-view classification technique named Multi-view Generalized Support Vector Machine via Mining the Inherent Relationship between Views (MRMvGSVM) for the application in face and smoke detection [10]. This technique utilizes multi-view learning in order to provide more accurate classification performance. The most important sample data were selected by multi-view regularization which helps in improving the classification accuracy and enhancing the robustness of the algorithm. To evaluate the performance of the model in multi-view smoke detection, the dataset proposed by Xu et al. [28] was used. The results showed a high mean smoke classification accuracy of 93.33% with a small standard deviation of 2.58, which is better that several other methods which were compared to the proposed method. This technique shows a high smoke detection accuracy, a fast operation, and an excellent stability, and is promising for the analysis of combustion-related applications.

VI. CONCLUSION AND FUTURE RECOMMENDATION

In this work, the application of various AI-enhanced visual inspection techniques for combustion flare analysis was reviewed. The progress in the application of RGB imaging, hyperspectral imaging, and multiview imaging for the analysis of gas flares was summarized and discussed. After reading the paper, readers can (a) have a comprehensive grasp of the present status of AI-aided visual inspection methods, particularly in the context of analyzing combustion flares. (b) They can also Understand the obstacles and constraints existing in this research domain, such as the absence of universally accessible datasets and the necessity for standardized performance assessment. (c) Moreover, they can find a summary of potential upcoming trends in this field including encompassing the utilization of deep learning approaches for hyperspectral image analysis and the creation of extensive benchmark datasets. The main conclusions of this survey are as follows:

- RGB imaging is an approachable technique for inspecting gas flares and several techniques were proposed in literature for obtaining useful information about the gas flare using RGB video stream. The main tasks were flare-related objects detection, flare-related objects

segmentation, and estimation of flaring performance measures. Deep learning techniques attracted the highest interest among researchers due to their high detection and segmentation accuracies.

- Hyperspectral imaging allows for detailed analysis of gas flare systems as it can measure various important flare parameters such as the combustion efficiency using the relative components amounts in the flare exhaust. The most used hyperspectral imagers for direct gas flare analysis are FTIR imagers due to their information-rich extracted data.
- Multi-view inspection of combustion flare is a technique used to observe and analyze flares and/or smoke emissions from multiple vantage points or angles. This approach involves the use of multiple cameras or sensors placed at strategic locations around a flare or smokestack, which allows for a more comprehensive and accurate analysis of the emissions. It can also provide a more complete understanding of the combustion process, including the size, shape, and intensity of the flame, the temperature and pressure of the gases, and the composition of the emissions. This information can be used to optimize the combustion process, improve efficiency, and reduce emissions of harmful hazards.
- A significant problem that slows down research on gas flare inspection is the lack of unified publicly-available datasets for comparing different flare analysis techniques and for evaluating the proposed novel techniques. Moreover, works on gas flare inspection use different performance measures which makes comparing their performance hard.

Although there have been a large number of studies that discussed the application of vision-based inspection for combustion flares analysis, there are still some critical topics that need to be investigated in the future to further improve the current technologies' analysis capabilities and accuracy. Here we present some discussions on future trends and emerging technologies in Gas Flares inspection:

- Deep Learning for hyper-spectral data analysis: Despite the wide application of deep learning techniques in the analysis of combustion flares using RGB images, there have been no works that discuss the application of deep learning techniques for the analysis of hyperspectral images of flares. Deep learning has shown huge potential in the analysis of hyperspectral data [138], [171], [172], [173], [174]. Therefore, we highly recommend studies that use various deep-learning analysis techniques of hyperspectral imagery for the analysis of gas flares.
- Gas Flares-oriented Vision Transformer: Vision Transformers (ViT) [23] are a novel type of deep learning models that have shown huge potential in various computer vision tasks, such as detection and tracking [43], [175], [176], [177], [178]. ViTs have the benefits of efficiently extracting long-range dependencies between sequential data and can accurately detect large-scale dependencies between different parts of the image, making them of high potential for all types of image analysis tasks in general and visual flaring analysis tasks in specific. However, the progress made on implementing ViTs for gas flares analysis is extremely limited. Works that implement ViTs for various deep learning-based analysis tasks of industrial flares such as smoke detection, soot detection, and real-time monitoring are highly recommended as they could outperform the currently used deep learning methods. Besides, ViT itself can also work as one efficient block of a deeper neural network. There are existing works that use ViT as a feature extractor and interpret extracted information with extra mechanisms like 'quadrangle attention' [179], 'super token sampling' [180], these works give hints to Gas Flares-related tasks on how to improve the model performance. Some other works process ViT-extracted features with specialized structures such as BLSTM [181] to finish a prediction task, this could inspire indicator prediction tasks in Gas Flares measurement. Moreover, the use of ViTs for the analysis of hyperspectral image data was carried out in literature [182], [183], [184] and the application of this method for gas flare analysis is a very important topic to be investigated.
- Unified public data set construction: Even though there are several datasets available online for flame and smoke detection in RGB images [14], [16], [25], there is no unified benchmarking dataset that can be used to compare the performance of novel detection or segmentation algorithms. To evaluate and compare the performance of various approaches, unified datasets for detection and segmentation benchmarking are therefore essential. Moreover, public datasets on multi-spectral and hyper-spectral imaging of typical flare scenes (flame and smoke scenes) are very limited and insufficient. Similarly, there is no publicly available dataset designed for evaluating and benchmarking multi-view flare analysis techniques. The presence of such datasets will increase the research interest in the realm and also make this field easier to incorporate up-to-date technologies such as Language-Image Contrastive Learning which has new requirements on the data format.
- The standardization of evaluation metrics: There is a wide variety of performance measures that were used to evaluate detection and segmentation methods in the literature. Likewise, in the case of combustion flare inspection methods, published works used different evaluation measures which makes it hard to compare the performance of different methods. Thus, unified performance measures on unified benchmarking datasets are required to be reported by novel works for comparison with other techniques in the literature.

ACKNOWLEDGMENT

(Muaz Al Radi and Pengfei Li contributed equally to this work.)

REFERENCES

[1] M. K. Alradi, "Autonomous inspection of flare stacks using a visual servoing controlled unmanned aerial vehicle (UAV)," Khalifa Univ., Abu Dhabi, UAE, Tech. Rep. 100059660, 2022.

[2] M. A. Radi, H. Karki, N. Werghi, S. Javed, and J. Dias, "Vision-based inspection of flare stacks operation using a visual servoing controlled autonomous unmanned aerial vehicle (UAV)," in *Proc. 48th Annu. Conf. IEEE Ind. Electron. Soc.*, Oct. 2022, pp. 1–6.

[3] R. Panfili, "High-fidelity forward model for determining combustion efficiency of industrial flares," in *Proc. 6th Workshop Hyperspectral Image Signal Process., Evol. Remote Sens. (WHISPERS)*, Jun. 2014, pp. 1–4.

[4] T. Xuan Truong and J.-M. Kim, "Fire flame detection in video sequences using multi-stage pattern recognition techniques," *Eng. Appl. Artif. Intell.*, vol. 25, no. 7, pp. 1365–1372, Oct. 2012.

[5] J. Smart, G. Lu, Y. Yan, and G. Riley, "Characterisation of an oxy-coal flame through digital imaging," *Combustion Flame*, vol. 157, no. 6, pp. 1132–1139, Jun. 2010.

[6] L. Arias, S. Torres, D. Sbarbaro, and P. Ngendakumana, "On the spectral bands measurements for combustion monitoring," *Combustion Flame*, vol. 158, no. 3, pp. 423–433, Mar. 2011.

[7] L. Huang, G. Liu, Y. Wang, H. Yuan, and T. Chen, "Fire detection in video surveillances using convolutional neural networks and wavelet transform," *Eng. Appl. Artif. Intell.*, vol. 110, Apr. 2022, Art. no. 104737.

[8] A. Gaur, A. Singh, A. Kumar, A. Kumar, and K. Kapoor, "Video flame and smoke based fire detection algorithms: A literature review," *Fire Technol.*, vol. 56, no. 5, pp. 1943–1980, Sep. 2020.

[9] M. Faruolo, A. Caseiro, T. Lacava, and J. W. Kaiser, "Gas flaring: A review focused on its analysis from space," *IEEE Geosci. Remote Sens. Mag.*, vol. 9, no. 1, pp. 258–281, Mar. 2021.

[10] M. A. Radi, P. Li, H. Karki, N. Werghi, S. Javed, and J. Dias, "Multi-view inspection of flare stacks operation using a vision-controlled autonomous UAV," in *Proc. 49th Annu. Conf. IEEE Ind. Electron. Soc.*, Oct. 2023, pp. 1–6.

[11] X. Xie, K. Gu, and J. Qiao, "A new anomaly detector of flare pilot based on Siamese network," in *Proc. Chin. Autom. Congr. (CAC)*, Nov. 2020, pp. 1–12.

[12] Y. Zeng, J. Morris, and M. Dombrowski, "Validation of a new method for measuring and continuously monitoring the efficiency of industrial flares," *J. Air Waste Manage. Assoc.*, vol. 66, no. 1, pp. 76–86, Jan. 2016.

[13] A. Cellier, C. J. Lapeyre, G. Öztarlik, T. Poinsot, T. Schuller, and L. Selle, "Detection of precursors of combustion instability using convolutional recurrent neural networks," *Combustion Flame*, vol. 233, Nov. 2021, Art. no. 111558.

[14] Y. H. Habiboğlu, O. Günay, and A. E. Çetin, "Covariance matrix-based fire and flame detection method in video," *Mach. Vis. Appl.*, vol. 23, no. 6, pp. 1103–1113, Nov. 2012.

[15] R. Vezzani and R. Cucchiara, "Video surveillance online repository (ViSOR): An integrated framework," *Multimedia Tools Appl.*, vol. 50, no. 2, pp. 359–380, Nov. 2010.

[16] D. Y. T. Chino, L. P. S. Avalhais, J. F. Rodrigues, and A. J. M. Traina, "BoWFire: Detection of fire in still images by integrating pixel color and texture analysis," in *Proc. 28th SIBGRAPI Conf. Graph., Patterns Images*, Aug. 2015, pp. 95–102.

[17] F. Yuan, Z. Fang, S. Wu, Y. Yang, and Y. Fang, "Real-time image smoke detection using staircase searching-based dual threshold AdaBoost and dynamic analysis," *IET Image Process.*, vol. 9, no. 10, pp. 849–856, Oct. 2015.

[18] K. Muhammad, S. Khan, V. Palade, I. Mehmood, and V. H. C. de Albuquerque, "Edge intelligence-assisted smoke detection in foggy surveillance environments," *IEEE Trans. Ind. Informat.*, vol. 16, no. 2, pp. 1067–1075, Feb. 2020.

[19] S. Khan, K. Muhammad, S. Mumtaz, S. W. Baik, and V. H. C. de Albuquerque, "Energy-efficient deep CNN for smoke detection in foggy IoT environment," *IEEE Internet Things J.*, vol. 6, no. 6, pp. 9237–9245, Dec. 2019.

[20] P. Foggia, A. Saggese, and M. Vento, "Real-time fire detection for video-surveillance applications using a combination of experts based on color, shape, and motion," *IEEE Trans. Circuits Syst. Video Technol.*, vol. 25, no. 9, pp. 1545–1556, Sep. 2015.

[21] T. Toulouse, L. Rossi, A. Campana, T. Celik, and M. A. Akhloufi, "Computer vision for wildfire research: An evolving image dataset for processing and analysis," *Fire Saf. J.*, vol. 92, pp. 188–194, Sep. 2017.

[22] A. Radford, J. W. Kim, C. Hallacy, A. Ramesh, G. Goh, S. Agarwal, G. Sastry, A. Askell, P. Mishkin, and J. Clark, "Learning transferable visual models from natural language supervision," in *Proc. Int. Conf. Mach. Learn.*, vol. 139, 2021, pp. 8748–8763.

[23] A. Dosovitskiy, L. Beyer, A. Kolesnikov, D. Weissenborn, X. Zhai, T. Unterthiner, M. Dehghani, M. Minderer, G. Heigold, S. Gelly, J. Uszkoreit, and N. Houlsby, "An image is worth 16×16 words: Transformers for image recognition at scale," 2020, *arXiv:2010.11929*.

[24] B. C. Ko, S. J. Ham, and J. Y. Nam, "Modeling and formalization of fuzzy finite automata for detection of irregular fire flames," *IEEE Trans. Circuits Syst. Video Technol.*, vol. 21, no. 12, pp. 1903–1912, Dec. 2011.

[25] M. T. Cazzolato, L. Avalhais, D. Chino, J. S. Ramos, J. A. de Souza, J. F. Rodrigues, and A. Traina, "FISMO: A compilation of datasets from emergency situations for fire and smoke analysis," in *Proc. Brazilian Symp. Databases*, 2017, pp. 213–223.

[26] J. Mlích, K. Koplík, M. Hradiš, and P. Zemčík, "Fire segmentation in still images," in *Proc. Int. Conf. Adv. Concepts Intell. Vis. Syst.* Cham, Switzerland: Springer, 2020, pp. 27–37.

[27] Z. Yin, B. Wan, F. Yuan, X. Xia, and J. Shi, "A deep normalization and convolutional neural network for image smoke detection," *IEEE Access*, vol. 5, pp. 18429–18438, 2017.

[28] G. Xu, Y. Zhang, Q. Zhang, G. Lin, and J. Wang, "Deep domain adaptation based video smoke detection using synthetic smoke images," *Fire Saf. J.*, vol. 93, pp. 53–59, Oct. 2017.

[29] S. Khan, K. Muhammad, T. Hussain, J. D. Ser, F. Cuzzolin, S. Bhattacharyya, Z. Akhtar, and V. H. C. de Albuquerque, "DeepSmoke: Deep learning model for smoke detection and segmentation in outdoor environments," *Expert Syst. Appl.*, vol. 182, Nov. 2021, Art. no. 115125.

[30] S. Aslan, U. Güdükbay, B. U. Töreyin, and A. E. Çetin, "Deep convolutional generative adversarial networks based flame detection in video," 2019, *arXiv:1902.01824*.

[31] T. T. Verlekar and A. Bernardino, "Video based fire detection using xception and Conv-LSTM," in *Proc. 15th Int. Symp. Adv. Vis. Comput.*, San Diego, CA, USA. Cham, Switzerland: Springer, 2020, pp. 277–285.

[32] F. Chollet, "Xception: Deep learning with depthwise separable convolutions," in *Proc. IEEE Conf. Comput. Vis. Pattern Recognit. (CVPR)*, Jul. 2017, pp. 1800–1807.

[33] M. Shahid and K.-L. Hua, "Fire detection using transformer network," in *Proc. Int. Conf. Multimedia Retr.*, Aug. 2021, pp. 627–630.

[34] A. J. Dunnings and T. P. Breckon, "Experimentally defined convolutional neural network architecture variants for non-temporal real-time fire detection," in *Proc. 25th IEEE Int. Conf. Image Process. (ICIP)*, Oct. 2018, pp. 1558–1562.

[35] K. Muhammad, J. Ahmad, Z. Lv, P. Bellavista, P. Yang, and S. W. Baik, "Efficient deep CNN-based fire detection and localization in video surveillance applications," *IEEE Trans. Syst., Man, Cybern., Syst.*, vol. 49, no. 7, pp. 1419–1434, Jul. 2019.

[36] M. N. Favorskaya, "Early smoke detection in outdoor space: State-of-the-art, challenges and methods," in *Advances in Selected Artificial Intelligence Areas: World Outstanding Women in Artificial Intelligence*. Cham, Switzerland: Springer, 2022, pp. 171–208.

[37] Y. Wang, C. Hua, W. Ding, and R. Wu, "Real-time detection of flame and smoke using an improved YOLOv4 network," *Signal, Image Video Process.*, vol. 16, no. 4, pp. 1109–1116, Jun. 2022.

[38] Y. Peng and Y. Wang, "Real-time forest smoke detection using hand-designed features and deep learning," *Comput. Electron. Agricult.*, vol. 167, Dec. 2019, Art. no. 105029.

[39] S.-Y. Kim and A. Muminov, "Forest fire smoke detection based on deep learning approaches and unmanned aerial vehicle images," *Sensors*, vol. 23, no. 12, p. 5702, Jun. 2023.

[40] M. Masoom S., Q. Zhang, P. Dai, Y. Jia, Y. Zhang, J. Zhu, and J. Wang, "Early smoke detection based on improved YOLO-PCA network," *Fire*, vol. 5, no. 2, p. 40, Mar. 2022.

[41] Z. Zhang, X. Lu, G. Cao, Y. Yang, L. Jiao, and F. Liu, "ViT-YOLO: Transformer-based YOLO for object detection," in *Proc. IEEE/CVF Int. Conf. Comput. Vis. Workshops (ICCVW)*, Oct. 2021, pp. 2799–2808.
[42] G. Jocher. (Jan. 2023). *Ultralytics/YOLOv5: V3.1—Bug Fixes and Performance Improvements*. [Online]. Available: https://github.com/ultralytics/ultralytics
[43] N. Carion, F. Massa, G. Synnaeve, N. Usunier, A. Kirillov, and S. Zagoruyko, "End-to-end object detection with transformers," in *Proc. Eur. Conf. Comput. Vis.* Cham, Switzerland: Springer, 2020, pp. 213–229.
[44] A. Yazdi, H. Qin, C. B. Jordan, L. Yang, and F. Yan, "Nemo: An open-source transformer-supercharged benchmark for fine-grained wildfire smoke detection," *Remote Sens.*, vol. 14, no. 16, p. 3979, Aug. 2022.
[45] W. Weng, Y. Zhang, and Z. Xiong, "Event-based video reconstruction using transformer," in *Proc. IEEE/CVF Int. Conf. Comput. Vis. (ICCV)*, Oct. 2021, pp. 2543–2552.
[46] Y. Peng, Y. Zhang, Z. Xiong, X. Sun, and F. Wu, "GET: Group event transformer for event-based vision," in *Proc. IEEE/CVF Int. Conf. Comput. Vis. (ICCV)*, Oct. 2023, pp. 6038–6048.
[47] S. Chaturvedi, P. Khanna, and A. Ojha, "A survey on vision-based outdoor smoke detection techniques for environmental safety," *ISPRS J. Photogramm. Remote Sens.*, vol. 185, pp. 158–187, Mar. 2022.
[48] B. Liu, B. Sun, P. Cheng, and Y. Huang, "An embedded portable lightweight platform for real-time early smoke detection," *Sensors*, vol. 22, no. 12, p. 4655, Jun. 2022.
[49] Y. Jia, H. Du, H. Wang, R. Yu, L. Fan, G. Xu, and Q. Zhang, "Automatic early smoke segmentation based on conditional generative adversarial networks," *Optik*, vol. 193, Sep. 2019, Art. no. 162879.
[50] L. Zhao, J. Liu, S. Peters, J. Li, S. Oliver, and N. Mueller, "Investigating the impact of using IR bands on early fire smoke detection from landsat imagery with a lightweight CNN model," *Remote Sens.*, vol. 14, no. 13, p. 3047, Jun. 2022.
[51] D. Xiong and L. Yan, "Early smoke detection of forest fires based on SVM image segmentation," *J. Forest Sci.*, vol. 65, no. 4, pp. 150–159, Apr. 2019.
[52] K. He, X. Zhang, S. Ren, and J. Sun, "Deep residual learning for image recognition," in *Proc. IEEE Conf. Comput. Vis. Pattern Recognit. (CVPR)*, Jun. 2016, pp. 770–778.
[53] V. E. Sathishkumar, J. Cho, M. Subramanian, and O. S. Naren, "Forest fire and smoke detection using deep learning-based learning without forgetting," *Fire Ecology*, vol. 19, no. 1, pp. 1–17, Feb. 2023.
[54] K. Simonyan and A. Zisserman, "Very deep convolutional networks for large-scale image recognition," 2014, *arXiv:1409.1556*.
[55] M. D. Zeiler and R. Fergus, "Visualizing and understanding convolutional networks," in *Proc. Eur. Conf. Comput. Vis.* Cham, Switzerland: Springer, 2014, pp. 818–833.
[56] A. Krizhevsky, I. Sutskever, and G. E. Hinton, "ImageNet classification with deep convolutional neural networks," in *Proc. Adv. Neural Inf. Process. Syst. (NIPS)*, 2012, pp. 1097–1105.
[57] F. Yuan, J. Shi, X. Xia, Y. Fang, Z. Fang, and T. Mei, "High-order local ternary patterns with locality preserving projection for smoke detection and image classification," *Inf. Sci.*, vol. 372, pp. 225–240, Dec. 2016.
[58] S. R. Dubey, S. K. Singh, and R. K. Singh, "Multichannel decoded local binary patterns for content-based image retrieval," *IEEE Trans. Image Process.*, vol. 25, no. 9, pp. 4018–4032, Sep. 2016.
[59] K. Gu, Z. Xia, J. Qiao, and W. Lin, "Deep dual-channel neural network for image-based smoke detection," *IEEE Trans. Multimedia*, vol. 22, no. 2, pp. 311–323, Feb. 2020.
[60] G. Huang, Z. Liu, L. Van Der Maaten, and K. Q. Weinberger, "Densely connected convolutional networks," in *Proc. IEEE Conf. Comput. Vis. Pattern Recognit. (CVPR)*, Jul. 2017, pp. 2261–2269.
[61] C. Szegedy, W. Liu, Y. Jia, P. Sermanet, S. Reed, D. Anguelov, D. Erhan, V. Vanhoucke, and A. Rabinovich, "Going deeper with convolutions," in *Proc. IEEE Conf. Comput. Vis. Pattern Recognit. (CVPR)*, Jun. 2015, pp. 1–9.
[62] K. Gu, Y. Zhang, and J. Qiao, "Vision-based monitoring of flare soot," *IEEE Trans. Instrum. Meas.*, vol. 69, no. 9, pp. 7136–7145, Sep. 2020.
[63] X. Hou, J. Harel, and C. Koch, "Image signature: Highlighting sparse salient regions," *IEEE Trans. Pattern Anal. Mach. Intell.*, vol. 34, no. 1, pp. 194–201, Jan. 2012.
[64] A. G. Howard, M. Zhu, B. Chen, D. Kalenichenko, W. Wang, T. Weyand, M. Andreetto, and H. Adam, "MobileNets: Efficient convolutional neural networks for mobile vision applications," 2017, *arXiv:1704.04861*.
[65] K. Zhou, J. Yang, C. C. Loy, and Z. Liu, "Conditional prompt learning for vision-language models," in *Proc. IEEE/CVF Conf. Comput. Vis. Pattern Recognit. (CVPR)*, Jun. 2022, pp. 16795–16804.
[66] G. Li and J. J. Jung, "Deep learning for anomaly detection in multivariate time series: Approaches, applications, and challenges," *Inf. Fusion*, vol. 91, pp. 93–102, Mar. 2023.
[67] J. Liu, G. Xie, J. Wang, S. Li, C. Wang, F. Zheng, and Y. Jin, "Deep industrial image anomaly detection: A survey," *Mach. Intell. Res.*, vol. 21, no. 1, pp. 104–135, Feb. 2024.
[68] S. Fu, X. Gao, F. Zhai, B. Li, B. Xue, J. Yu, Z. Meng, and G. Zhang, "A time series anomaly detection method based on series-parallel transformers with spatial and temporal association discrepancies," *Inf. Sci.*, vol. 657, Feb. 2024, Art. no. 119978.
[69] I. Mackey, R. Chimni, and J. Su, "Early detection of temporal constraint violations," *Inf. Comput.*, vol. 296, Jan. 2024, Art. no. 105114.
[70] Y. Luo, L. Zhao, P. Liu, and D. Huang, "Fire smoke detection algorithm based on motion characteristic and convolutional neural networks," *Multimedia Tools Appl.*, vol. 77, no. 12, pp. 15075–15092, Jun. 2018.
[71] G. Lin, Y. Zhang, G. Xu, and Q. Zhang, "Smoke detection on video sequences using 3D convolutional neural networks," *Fire Technol.*, vol. 55, no. 5, pp. 1827–1847, Sep. 2019.
[72] S. Ye, Z. Bai, H. Chen, R. Bohush, and S. Ablameyko, "An effective algorithm to detect both smoke and flame using color and wavelet analysis," *Pattern Recognit. Image Anal.*, vol. 27, no. 1, pp. 131–138, Jan. 2017.
[73] D. K. Appana, R. Islam, S. A. Khan, and J.-M. Kim, "A video-based smoke detection using smoke flow pattern and spatial–temporal energy analyses for alarm systems," *Inf. Sci.*, vols. 418–419, pp. 91–101, Dec. 2017.
[74] R. Chi, Z. Lu, and Q. Ji, "Real-time multi-feature based fire flame detection in video," *IET Image Process.*, vol. 11, no. 1, pp. 31–37, Jan. 2017.
[75] T. W. Hsu, S. Pare, M. S. Meena, D. K. Jain, D. L. Li, A. Saxena, M. Prasad, and C. T. Lin, "An early flame detection system based on image block threshold selection using knowledge of local and global feature analysis," *Sustainability*, vol. 12, no. 21, p. 8899, Oct. 2020.
[76] C. Emmy Prema, S. S. Vinsley, and S. Suresh, "Efficient flame detection based on static and dynamic texture analysis in forest fire detection," *Fire Technol.*, vol. 54, no. 1, pp. 255–288, Jan. 2018.
[77] X.-F. Han, J. S. Jin, M.-J. Wang, W. Jiang, L. Gao, and L.-P. Xiao, "Video fire detection based on Gaussian mixture model and multi-color features," *Signal, Image Video Process.*, vol. 11, no. 8, pp. 1419–1425, Nov. 2017.
[78] X. Wang, Y. Li, and Z. Li, "Research on flame detection algorithm based on multi–feature fusion," in *Proc. IEEE 4th Inf. Technol., Netw., Electron. Autom. Control Conf. (ITNEC)*, vol. 1, Jun. 2020, pp. 184–189.
[79] Z. Zhong, M. Wang, Y. Shi, and W. Gao, "A convolutional neural network-based flame detection method in video sequence," *Signal, Image Video Process.*, vol. 12, no. 8, pp. 1619–1627, Nov. 2018.
[80] K. Muhammad, J. Ahmad, I. Mehmood, S. Rho, and S. W. Baik, "Convolutional neural networks based fire detection in surveillance videos," *IEEE Access*, vol. 6, pp. 18174–18183, 2018.
[81] J. Ryu and D. Kwak, "Flame detection using appearance-based pre-processing and convolutional neural network," *Appl. Sci.*, vol. 11, no. 11, p. 5138, May 2021.
[82] N. Yu and Y. Chen, "Video flame detection method based on TwoStream convolutional neural network," in *Proc. IEEE 8th Joint Int. Inf. Technol. Artif. Intell. Conf. (ITAIC)*, May 2019, pp. 482–486.
[83] A. Filonenko, D. C. Hernández, and K.-H. Jo, "Fast smoke detection for video surveillance using CUDA," *IEEE Trans. Ind. Informat.*, vol. 14, no. 2, pp. 725–733, Feb. 2018.
[84] X. Wu, X. Lu, and H. Leung, "A motion and lightness saliency approach for forest smoke segmentation and detection," *Multimedia Tools Appl.*, vol. 79, nos. 1–2, pp. 69–88, Jan. 2020.

[85] N. Alamgir, K. Nguyen, V. Chandran, and W. Boles, "Combining multi-channel color space with local binary co-occurrence feature descriptors for accurate smoke detection from surveillance videos," *Fire Saf. J.*, vol. 102, pp. 1–10, Dec. 2018.

[86] H. Tian, W. Li, P. O. Ogunbona, and L. Wang, "Detection and separation of smoke from single image frames," *IEEE Trans. Image Process.*, vol. 27, no. 3, pp. 1164–1177, Mar. 2018.

[87] F. Yuan, X. Xia, J. Shi, H. Li, and G. Li, "Non-linear dimensionality reduction and Gaussian process based classification method for smoke detection," *IEEE Access*, vol. 5, pp. 6833–6841, 2017.

[88] X. Wu, X. Lu, and H. Leung, "A video based fire smoke detection using robust AdaBoost," *Sensors*, vol. 18, no. 11, p. 3780, Nov. 2018.

[89] Y. Hu and X. Lu, "Real-time video fire smoke detection by utilizing spatial–temporal ConvNet features," *Multimedia Tools Appl.*, vol. 77, no. 22, pp. 29283–29301, Nov. 2018.

[90] H. Liu, F. Lei, C. Tong, C. Cui, and L. Wu, "Visual smoke detection based on ensemble deep CNNs," *Displays*, vol. 69, Sep. 2021, Art. no. 102020.

[91] Y. Jia, W. Chen, M. Yang, L. Wang, D. Liu, and Q. Zhang, "Video smoke detection with domain knowledge and transfer learning from deep convolutional neural networks," *Optik*, vol. 240, Aug. 2021, Art. no. 166947.

[92] Q.-X. Zhang, G.-H. Lin, Y.-M. Zhang, G. Xu, and J.-J. Wang, "Wildland forest fire smoke detection based on faster R-CNN using synthetic smoke images," *Proc. Eng.*, vol. 211, pp. 441–446, Jan. 2018.

[93] Y. Cao, F. Yang, Q. Tang, and X. Lu, "An attention enhanced bidirectional LSTM for early forest fire smoke recognition," *IEEE Access*, vol. 7, pp. 154732–154742, 2019.

[94] R. Kaabi, M. Sayadi, M. Bouchouicha, F. Fnaiech, E. Moreau, and J. M. Ginoux, "Early smoke detection of forest wildfire video using deep belief network," in *Proc. 4th Int. Conf. Adv. Technol. Signal Image Process. (ATSIP)*, Mar. 2018, pp. 1–6.

[95] R. Kaabi, M. Bouchouicha, A. Mouelhi, M. Sayadi, and E. Moreau, "An efficient smoke detection algorithm based on deep belief network classifier using energy and intensity features," *Electronics*, vol. 9, no. 9, p. 1390, Aug. 2020.

[96] G. Xu, Y. Zhang, Q. Zhang, G. Lin, Z. Wang, Y. Jia, and J. Wang, "Video smoke detection based on deep saliency network," *Fire Saf. J.*, vol. 105, pp. 277–285, Apr. 2019.

[97] M. Yin, C. Lang, Z. Li, S. Feng, and T. Wang, "Recurrent convolutional network for video-based smoke detection," *Multimedia Tools Appl.*, vol. 78, no. 1, pp. 237–256, Jan. 2019.

[98] H.-S. Choi, M. Jeon, K. Song, and M. Kang, "Semantic fire segmentation model based on convolutional neural network for outdoor image," *Fire Technol.*, vol. 57, no. 6, pp. 3005–3019, Nov. 2021.

[99] V. S. Bochkov and L. Y. Kataeva, "WUUNet: Advanced fully convolutional neural network for multiclass fire segmentation," *Symmetry*, vol. 13, no. 1, p. 98, Jan. 2021.

[100] M. Tan and Q. Le, "EfficientNet: Rethinking model scaling for convolutional neural networks," in *Proc. Int. Conf. Mach. Learn.*, 2019, pp. 6105–6114.

[101] L.-C. Chen, Y. Zhu, G. Papandreou, F. Schroff, and H. Adam, "Encoder–decoder with atrous separable convolution for semantic image segmentation," in *Proc. Eur. Conf. Comput. Vis. (ECCV)*, 2018, pp. 801–818.

[102] M. Sandler, A. Howard, M. Zhu, A. Zhmoginov, and L.-C. Chen, "MobileNetV2: Inverted residuals and linear bottlenecks," in *Proc. IEEE/CVF Conf. Comput. Vis. Pattern Recognit.*, Jun. 2018, pp. 4510–4520.

[103] H. Noh, S. Hong, and B. Han, "Learning deconvolution network for semantic segmentation," in *Proc. IEEE Int. Conf. Comput. Vis. (ICCV)*, Dec. 2015, pp. 1520–1528.

[104] J. Long, E. Shelhamer, and T. Darrell, "Fully convolutional networks for semantic segmentation," in *Proc. IEEE Conf. Comput. Vis. Pattern Recognit. (CVPR)*, Jun. 2015, pp. 3431–3440.

[105] L.-C. Chen, G. Papandreou, I. Kokkinos, K. Murphy, and A. L. Yuille, "DeepLab: Semantic image segmentation with deep convolutional nets, atrous convolution, and fully connected CRFs," *IEEE Trans. Pattern Anal. Mach. Intell.*, vol. 40, no. 4, pp. 834–848, Apr. 2018.

[106] V. Badrinarayanan, A. Kendall, and R. Cipolla, "SegNet: A deep convolutional encoder–decoder architecture for image segmentation," *IEEE Trans. Pattern Anal. Mach. Intell.*, vol. 39, no. 12, pp. 2481–2495, Dec. 2017.

[107] S. Frizzi, M. Bouchouicha, J. Ginoux, E. Moreau, and M. Sayadi, "Convolutional neural network for smoke and fire semantic segmentation," *IET Image Process.*, vol. 15, no. 3, pp. 634–647, Feb. 2021.

[108] F. Yuan, L. Zhang, X. Xia, B. Wan, Q. Huang, and X. Li, "Deep smoke segmentation," *Neurocomputing*, vol. 357, pp. 248–260, Sep. 2019.

[109] O. Ronneberger, P. Fischer, and T. Brox, "U-Net: Convolutional networks for biomedical image segmentation," in *Proc. 18th Int. Conf. Med. Image Comput. Comput.-Assist. Intervent.*, vol. 9351. Cham, Switzerland: Springer, 2015, pp. 234–241.

[110] B. M. Nogueira de Souza and J. Facon, "A fire color mapping-based segmentation: Fire pixel segmentation approach," in *Proc. IEEE/ACS 13th Int. Conf. Comput. Syst. Appl. (AICCSA)*, Nov. 2016, pp. 1–8.

[111] T. Toulouse, L. Rossi, M. Akhloufi, T. Celik, and X. Maldague, "Benchmarking of wildland fire colour segmentation algorithms," *IET Image Process.*, vol. 9, no. 12, pp. 1064–1072, Dec. 2015.

[112] A. Khatami, S. Mirghasemi, A. Khosravi, C. P. Lim, and S. Nahavandi, "A new PSO-based approach to fire flame detection using K-medoids clustering," *Expert Syst. Appl.*, vol. 68, pp. 69–80, Feb. 2017.

[113] Y. Zhao, "Candidate smoke region segmentation of fire video based on rough set theory," *J. Electr. Comput. Eng.*, vol. 2015, pp. 1–8, Jan. 2015.

[114] Q. Li, H. Liu, J. Zhang, and P. Zeng, "Target segmentation of industrial smoke image based on LBP silhouettes coefficient variant (LBPSCV) algorithm," *IET Image Process.*, vol. 14, no. 12, pp. 2879–2889, Oct. 2020.

[115] Y. Jia, J. Yuan, J. Wang, J. Fang, Q. Zhang, and Y. Zhang, "A saliency-based method for early smoke detection in video sequences," *Fire Technol.*, vol. 52, no. 5, pp. 1271–1292, Sep. 2016.

[116] X. Li, Z. Chen, Q. M. J. Wu, and C. Liu, "3D parallel fully convolutional networks for real-time video wildfire smoke detection," *IEEE Trans. Circuits Syst. Video Technol.*, vol. 30, no. 1, pp. 89–103, Jan. 2020.

[117] J. Pan, X. Ou, and L. Xu, "A collaborative region detection and grading framework for forest fire smoke using weakly supervised fine segmentation and lightweight faster-RCNN," *Forests*, vol. 12, no. 6, p. 768, Jun. 2021.

[118] F. Yuan, L. Zhang, X. Xia, Q. Huang, and X. Li, "A wave-shaped deep neural network for smoke density estimation," *IEEE Trans. Image Process.*, vol. 29, pp. 2301–2313, 2020.

[119] G. Zhu, Z. Chen, C. Liu, X. Rong, and W. He, "3D video semantic segmentation for wildfire smoke," *Mach. Vis. Appl.*, vol. 31, no. 6, pp. 1–10, Sep. 2020.

[120] F. Yuan, L. Zhang, X. Xia, Q. Huang, and X. Li, "A gated recurrent network with dual classification assistance for smoke semantic segmentation," *IEEE Trans. Image Process.*, vol. 30, pp. 4409–4422, 2021.

[121] A. Garcia-Garcia, S. Orts-Escolano, S. Oprea, V. Villena-Martinez, P. Martinez-Gonzalez, and J. Garcia-Rodriguez, "A survey on deep learning techniques for image and video semantic segmentation," *Appl. Soft Comput.*, vol. 70, pp. 41–65, Sep. 2018.

[122] S. Minaee, Y. Boykov, F. Porikli, A. Plaza, N. Kehtarnavaz, and D. Terzopoulos, "Image segmentation using deep learning: A survey," *IEEE Trans. Pattern Anal. Mach. Intell.*, vol. 44, no. 7, pp. 3523–3542, Jul. 2022.

[123] E. Bourguignon, M. R. Johnson, and L. W. Kostiuk, "The use of a closed-loop wind tunnel for measuring the combustion efficiency of flames in a cross flow," *Combustion Flame*, vol. 119, no. 3, pp. 319–334, Nov. 1999.

[124] M. Dai, B. Zhou, J. Zhang, R. Cheng, Q. Liu, R. Zhao, B. Wang, and B. Gao, "3-D soot temperature and volume fraction reconstruction of afterburner flame via deep learning algorithms," *Combustion Flame*, vol. 252, Jun. 2023, Art. no. 112743.

[125] M. R. Johnson, R. W. Devillers, and K. A. Thomson, "Quantitative field measurement of soot emission from a large gas flare using sky-LOSA," *Environ. Sci. Technol.*, vol. 45, no. 1, pp. 345–350, Jan. 2011.

[126] D. Castiñeira, B. C. Rawlings, and T. F. Edgar, "Multivariate image analysis (MIA) for industrial flare combustion control," *Ind. Eng. Chem. Res.*, vol. 51, no. 39, pp. 12642–12652, Oct. 2012.

[127] K. Gu, Y. Zhang, and J. Qiao, "Ensemble meta-learning for few-shot soot density recognition," *IEEE Trans. Ind. Informat.*, vol. 17, no. 3, pp. 2261–2270, Mar. 2021.

[128] Q. Dai, J.-H. Cheng, D.-W. Sun, and X.-A. Zeng, "Advances in feature selection methods for hyperspectral image processing in food industry applications: A review," *Crit. Rev. Food Sci. Nutrition*, vol. 55, no. 10, pp. 1368–1382, Aug. 2015.

[129] D. Liu, D.-W. Sun, and X.-A. Zeng, "Recent advances in wavelength selection techniques for hyperspectral image processing in the food industry," *Food Bioprocess Technol.*, vol. 7, no. 2, pp. 307–323, Feb. 2014.

[130] L. D. Medus, M. Saban, J. V. Francés-Víllora, M. Bataller-Mompeán, and A. Rosado-Muñoz, "Hyperspectral image classification using CNN: Application to industrial food packaging," *Food Control*, vol. 125, Jul. 2021, Art. no. 107962.

[131] B. Lu, P. Dao, J. Liu, Y. He, and J. Shang, "Recent advances of hyperspectral imaging technology and applications in agriculture," *Remote Sens.*, vol. 12, no. 16, p. 2659, Aug. 2020.

[132] T. Adão, J. HruŠka, L. Pádua, J. Bessa, E. Peres, R. Morais, and J. Sousa, "Hyperspectral imaging: A review on UAV-based sensors, data processing and applications for agriculture and forestry," *Remote Sens.*, vol. 9, no. 11, p. 1110, Oct. 2017.

[133] M. B. Stuart, A. J. S. McGonigle, and J. R. Willmott, "Hyperspectral imaging in environmental monitoring: A review of recent developments and technological advances in compact field deployable systems," *Sensors*, vol. 19, no. 14, p. 3071, Jul. 2019.

[134] G. Lu and B. Fei, "Medical hyperspectral imaging: A review," *J. Biomed. Opt.*, vol. 19, no. 1, Jan. 2014, Art. no. 010901.

[135] B. Fei, "Hyperspectral imaging in medical applications," in *Data Handling in Science and Technology*, vol. 32. Amsterdam, The Netherlands: Elsevier, 2020, pp. 523–565.

[136] G. Saiko, P. Lombardi, Y. Au, D. Queen, D. Armstrong, and K. Harding, "Hyperspectral imaging in wound care: A systematic review," *Int. Wound J.*, vol. 17, no. 6, pp. 1840–1856, Dec. 2020.

[137] X. Dong, M. Jakobi, S. Wang, M. H. Köhler, X. Zhang, and A. W. Koch, "A review of hyperspectral imaging for nanoscale materials research," *Appl. Spectrosc. Rev.*, vol. 54, no. 4, pp. 285–305, Apr. 2019.

[138] A. Signoroni, M. Savardi, A. Baronio, and S. Benini, "Deep learning meets hyperspectral image analysis: A multidisciplinary review," *J. Imag.*, vol. 5, no. 5, p. 52, May 2019.

[139] T. R. Blackwood, "An evaluation of flare combustion efficiency using open-path Fourier transform infrared technology," *J. Air Waste Manage. Assoc.*, vol. 50, no. 10, pp. 1714–1722, Oct. 2000.

[140] D. Leahey, M. Schroeder, and M. Hansen, "A theoretical assessment of flare efficiencies as a function of gas exit velocity and wind speed," in *Proc. Flaring Technol. Symp., Environ. Services Assoc. Alberta*, 1996, pp. 1–13.

[141] J. Wormhoudt, S. C. Herndon, J. Franklin, E. C. Wood, B. Knighton, S. Evans, C. Laush, M. Sloss, and R. Spellicy, "Comparison of remote sensing and extractive sampling measurements of flare combustion efficiency," *Ind. Eng. Chem. Res.*, vol. 51, no. 39, pp. 12621–12629, Oct. 2012.

[142] M.-A. Gagnon, P. Tremblay, S. Savary, P. Lagueux, and M. Chamberland, "Standoff thermal hyperspectral imaging for flare and smokestack characterization in industrial environments," in *Proc. 5th Workshop Hyperspectral Image Signal Process., Evol. Remote Sens. (WHISPERS)*, Jun. 2013, pp. 1–4, doi: 10.1109/WHISPERS.2013.8080745.

[143] A. Huot, M.-A. Gagnon, K.-A. Jahjah, P. Tremblay, S. Savary, V. Farley, P. Lagueux, É. Guyot, M. Chamberland, and F. Marcotte, "Time-resolved multispectral imaging of combustion reaction," *Proc. SPIE*, vol. 9485, Feb. 2015, Art. no. 94851C.

[144] Y. Zeng, J. Morris, and M. Dombrowski, "Multi-spectral infrared imaging system for flare combustion efficiency monitoring," U.S. Patent 9 258 495, Feb. 9, 2016.

[145] E. A. Moore, K. C. Gross, S. J. Bowen, G. P. Perram, M. Chamberland, V. Farley, J.-P. Gagnon, P. Lagueux, and A. Villemaire, "Characterizing and overcoming spectral artifacts in imaging Fourier-transform spectroscopy of turbulent exhaust plumes," *Proc. SPIE*, vol. 7304, Mar. 2009, Art. no. 730416, doi: 10.1117/12.818710.

[146] H. Dothe, J. Duff, J. Gruninger, P. Acharya, and A. Berk, "SAMM2, SHARC-4 and MODTRAN4 merged (user's manual)," Spectral Sci. Inc, Burlington, MA, USA, Rep., 2004.

[147] S. J. Grauer, B. M. Conrad, R. B. Miguel, and K. J. Daun, "Gaussian model for emission rate measurement of heated plumes using hyperspectral data," *J. Quant. Spectrosc. Radiat. Transf.*, vol. 206, pp. 125–134, Feb. 2018.

[148] R. Taylor and R. Panfili, "Utilizing hyperspectral imagery to identify highly-reactive volatile organic compounds in combustion flare emissions," in *Proc. 4th Workshop Hyperspectral Image Signal Process., Evol. Remote Sens. (WHISPERS)*, Jun. 2012, pp. 1–4.

[149] R. Panfili, P. Vujkovic-Cvijin, X. Tan, R. Kennett, R. Taylor, H. Dothe, and L. Bernstein, "Hyperspectral modeling of combustion flare emissions," in *Proc. Amer. Flame Res. Committee*, vol. 37, 2012.

[150] K. Han, W. Lee, and J. W. Hahn, "Effect of spectral line broadening and instrument function on the spectrum of a mid-infrared flare in a realistic environment," *Combustion Sci. Technol.*, vol. 188, no. 7, pp. 1152–1164, Jul. 2016.

[151] B. M. Conrad, J. N. Thornock, and M. R. Johnson, "Beam steering effects on remote optical measurements of pollutant emissions in heated plumes and flares," *J. Quant. Spectrosc. Radiat. Transf.*, vol. 254, Oct. 2020, Art. no. 107191.

[152] R. B. Miguel, J. Emmert, S. J. Grauer, J. N. Thornock, and K. J. Daun, "Optimal filter selection for quantitative gas mixture imaging," *J. Quant. Spectrosc. Radiat. Transf.*, vol. 254, Oct. 2020, Art. no. 107208.

[153] S. Chowdhury, T. Shipman, D. Chao, C. D. Elvidge, M. Zhizhin, and F.-C. Hsu, "Daytime gas flare detection using Landsat-8 multispectral data," in *Proc. IEEE Geosci. Remote Sens. Symp.*, Jul. 2014, pp. 258–261.

[154] S. Casadio, O. Arino, and D. Serpe, "Gas flaring monitoring from space using the ATSR instrument series," *Remote Sens. Environ.*, vol. 116, pp. 239–249, Jan. 2012.

[155] W. Schroeder, P. Oliva, L. Giglio, B. Quayle, E. Lorenz, and F. Morelli, "Active fire detection using Landsat-8/OLI data," *Remote Sens. Environ.*, vol. 185, pp. 210–220, Nov. 2016.

[156] C. Elvidge, M. Zhizhin, K. Baugh, F. Hsu, and T. Ghosh, "Extending nighttime combustion source detection limits with short wavelength VIIRS data," *Remote Sens.*, vol. 11, no. 4, p. 395, Feb. 2019.

[157] C. D. Elvidge, M. Zhizhin, F.-C. Hsu, and K. Baugh, "What is so great about nighttime VIIRS data for the detection and characterization of combustion sources?" *Proc. Asia–Pacific Adv. Netw.*, vol. 35, p. 33, Jun. 2013.

[158] C. Elvidge, M. Zhizhin, F.-C. Hsu, and K. Baugh, "VIIRS nightfire: Satellite pyrometry at night," *Remote Sens.*, vol. 5, no. 9, pp. 4423–4449, Sep. 2013.

[159] O. C. D. Anejionu, G. A. Blackburn, and J. D. Whyatt, "Detecting gas flares and estimating flaring volumes at individual flow stations using MODIS data," *Remote Sens. Environ.*, vol. 158, pp. 81–94, Mar. 2015.

[160] C. Elvidge, M. Zhizhin, K. Baugh, F.-C. Hsu, and T. Ghosh, "Methods for global survey of natural gas flaring from Visible Infrared Imaging Radiometer Suite data," *Energies*, vol. 9, no. 1, p. 14, Dec. 2015.

[161] M. Faruolo, T. Lacava, N. Pergola, and V. Tramutoli, "On the potential of the RST-FLARE algorithm for gas flaring characterization from space," *Sensors*, vol. 18, no. 8, p. 2466, Jul. 2018.

[162] M. Faruolo, T. Lacava, N. Pergola, and V. Tramutoli, "The VIIRS-based RST-FLARE configuration: The val d'Agri oil center gas flaring investigation in between 2015–2019," *Remote Sens.*, vol. 12, no. 5, p. 819, Mar. 2020.

[163] D. Fisher and M. J. Wooster, "Shortwave IR adaption of the mid-infrared radiance method of fire radiative power (FRP) retrieval for assessing industrial gas flaring output," *Remote Sens.*, vol. 10, no. 2, p. 305, Feb. 2018.

[164] M. Franklin, K. Chau, L. J. Cushing, and J. E. Johnston, "Characterizing flaring from unconventional oil and gas operations in south Texas using satellite observations," *Environ. Sci. Technol.*, vol. 53, no. 4, pp. 2220–2228, Feb. 2019.

[165] D. Zhang, C. Huang, J. Gu, J. Hou, Y. Zhang, W. Han, P. Dou, and Y. Feng, "Real-time wildfire detection algorithm based on VIIRS fire product and Himawari-8 data," *Remote Sens.*, vol. 15, no. 6, p. 1541, Mar. 2023.

[166] G. Chao, S. Sun, and J. Bi, "A survey on multiview clustering," *IEEE Trans. Artif. Intell.*, vol. 2, no. 2, pp. 146–168, Apr. 2021.

[167] X. Yan, S. Hu, Y. Mao, Y. Ye, and H. Yu, "Deep multi-view learning methods: A review," *Neurocomputing*, vol. 448, pp. 106–129, Aug. 2021.

[168] P. Li, Z. Zhang, A. S. Al-Sumaiti, N. Werghi, and C. Y. Yeun, "A robust adversary detection-deactivation method for metaverse-oriented collaborative deep learning," *IEEE Sensors J.*, 2024.

[169] S. Verstockt, S. Van Hoecke, N. Tilley, B. Merci, B. Sette, P. Lambert, C.-F.-J. Hollemeersch, and R. Van de Walle, "FireCube: A multi-view localization framework for 3D fire analysis," *Fire Saf. J.*, vol. 46, no. 5, pp. 262–275, Jul. 2011.

[170] Y. Cheng, L. Fu, P. Luo, Q. Ye, F. Liu, and W. Zhu, "Multi-view generalized support vector machine via mining the inherent relationship between views with applications to face and fire smoke recognition," *Knowl.-Based Syst.*, vol. 210, Dec. 2020, Art. no. 106488.
[171] S. Li, W. Song, L. Fang, Y. Chen, P. Ghamisi, and J. A. Benediktsson, "Deep learning for hyperspectral image classification: An overview," *IEEE Trans. Geosci. Remote Sens.*, vol. 57, no. 9, pp. 6690–6709, Sep. 2019.
[172] M. E. Paoletti, J. M. Haut, J. Plaza, and A. Plaza, "Deep learning classifiers for hyperspectral imaging: A review," *ISPRS J. Photogramm. Remote Sens.*, vol. 158, pp. 279–317, Dec. 2019.
[173] C. Chen, F. Jiang, C. Yang, S. Rho, W. Shen, S. Liu, and Z. Liu, "Hyperspectral classification based on spectral–spatial convolutional neural networks," *Eng. Appl. Artif. Intell.*, vol. 68, pp. 165–171, Feb. 2018.
[174] H. Zhou, X. Zhang, C. Zhang, and Q. Ma, "Quaternion convolutional neural networks for hyperspectral image classification," *Eng. Appl. Artif. Intell.*, vol. 123, Aug. 2023, Art. no. 106234.
[175] K. Han, Y. Wang, H. Chen, X. Chen, J. Guo, Z. Liu, Y. Tang, A. Xiao, C. Xu, Y. Xu, Z. Yang, Y. Zhang, and D. Tao, "A survey on visual transformer," 2020, *arXiv:2012.12556*.
[176] M. Zhao, K. Okada, and M. Inaba, "TrTr: Visual tracking with transformer," 2021, *arXiv:2105.03817*.
[177] X. Zhu, W. Su, L. Lu, B. Li, X. Wang, and J. Dai, "Deformable DETR: Deformable transformers for end-to-end object detection," 2020, *arXiv:2010.04159*.
[178] X. Chen, B. Yan, J. Zhu, D. Wang, X. Yang, and H. Lu, "Transformer tracking," in *Proc. IEEE/CVF Conf. Comput. Vis. Pattern Recognit. (CVPR)*, Jun. 2021, pp. 8122–8131.
[179] Q. Zhang, J. Zhang, Y. Xu, and D. Tao, "Vision transformer with quadrangle attention," *IEEE Trans. Pattern Anal. Mach. Intell.*, vol. 46, no. 5, pp. 3608–3624, May 2024.
[180] H. Huang, X. Zhou, J. Cao, R. He, and T. Tan, "Vision transformer with super token sampling," in *Proc. Conf. Comput. Vis. Pattern Recognit. (CVPR)*, Jun. 2023, pp. 22690–22699.
[181] L. Zhifeng, D. Feng, L. Jianyong, Z. Yue, and C. Hetao, "Comparison of BLSTM-attention and BLSTM-transformer models for wind speed prediction," *Proc. Bulgarian Acad. Sci.*, vol. 75, no. 1, pp. 80–89, Feb. 2022.
[182] X. He, Y. Chen, and Z. Lin, "Spatial-spectral transformer for hyperspectral image classification," *Remote Sens.*, vol. 13, no. 3, p. 498, Jan. 2021.
[183] D. Hong, Z. Han, J. Yao, L. Gao, B. Zhang, A. Plaza, and J. Chanussot, "SpectralFormer: Rethinking hyperspectral image classification with transformers," 2021, *arXiv:2107.02988*.
[184] X. He and Y. Chen, "Optimized input for CNN-based hyperspectral image classification using spatial transformer network," *IEEE Geosci. Remote Sens. Lett.*, vol. 16, no. 12, pp. 1884–1888, Dec. 2019.

MUAZ AL RADI received the B.Sc. degree in sustainable and renewable energy engineering from the University of Sharjah, Sharjah, United Arab Emirates, in 2020, and the M.Sc. degree in electrical and computer engineering from Khalifa University, Abu Dhabi, United Arab Emirates, in 2022, where he is currently pursuing the Ph.D. degree in electrical and computer engineering. He is also a Graduate Research and Teaching Assistant (GRTA). His research interests include computer vision, vision-based control, artificial intelligence (AI), and robotics.

PENGFEI LI received the B.Eng. degree (Hons.) in electronic and electrical engineering from the University of Glasgow (UOG), U.K., in 2022, and the B.Eng. degree in electronic and information engineering from the University of Electronic Science and Technology of China (UESTC), China, in 2022. He is currently pursuing the master's degree in electrical and computer engineering with Khalifa University of Science and Technology (KUST), United Arab Emirates, and the Ph.D. degree. His research interests include temporal event detection, multi-scenario segmentation, weakly-supervised anomaly detection, cryptography protocol, and language-image contrast learning.

SAID BOUMARAF received the Ph.D. degree from the School of Computer Science and Technology, Beijing Institute of Technology, China, in 2021. He was with Algerian Space Agency as a Chief Engineer and a Researcher for satellite communications. He is also a Postdoctoral Fellow with the Department of Computer Science, Khalifa University of Science and Technology, Abu Dhabi, United Arab Emirates. His research interests include AI for medical imaging, biometrics, computer vision, and machine learning.

JORGE DIAS (Senior Member, IEEE) received the Ph.D. degree in electrical engineering from the University of Coimbra, Coimbra, Portugal, in 1994. He coordinated the Artificial Perception Group, Institute of Systems and Robotics, University of Coimbra. He is currently a Full Professor with Khalifa University of Science and Technology, Abu Dhabi, United Arab Emirates, where he is also the Deputy Director of the Center of Autonomous Robotic Systems. His expertise is in the area of artificial perception (computer vision and robotic vision) and has contributed to the field, since 1984. He has been a principal investigator and a consortia coordinator for several research international projects and coordinates the research group on computer vision and artificial perception from Khalifa University Center for Autonomous Robotic Systems (KUCARS). He has published several articles in the area of computer vision and robotics include more than 300 publications in international journals and conference proceedings and recently published a book on probabilistic robot perception that addresses the use of statistical modeling and artificial intelligence for perception, planning, and decision in robots. He was the Project Coordinator of two European Consortium for the Projects "Social Robot" and "GrowMeUP" which were developed to support the inclusivity and well-being of the elderly generation.

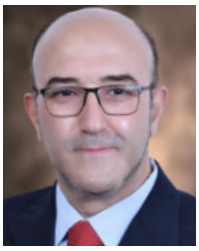

NAOUFEL WERGHI (Senior Member, IEEE) received the Ph.D. degree in computer vision from the University of Strasbourg, Strasbourg, France, in 1996. He was a Research Fellow with the Division of Informatics, The University of Edinburgh, Edinburgh, U.K., and a Lecturer with the Department of Computer Sciences, University of Glasgow, Glasgow, U.K. He was a Visiting Professor with the Department of Electrical and Computer Engineering, University of Louisville, Louisville, KY, USA. He is currently a Full Professor with the Department of Electrical and Computer Engineering, Khalifa University, Abu Dhabi, United Arab Emirates. His research interests include image analysis and interpretation, where he has been leading several funded projects in the areas of biometrics, medical imaging, and intelligent systems.

HAMAD KARKI received the bachelor's, master's, and Ph.D. degrees in engineering from Tokyo University of Technology. In 2008, he joined the Department of Mechanical Engineering, Khalifa University (former the Petroleum Institute), as an Assistant Professor, where he is currently an Associate Professor. He assumed his duties in research, teaching, and services. He enjoys teaching his classes as well as mentoring senior design projects every year. He served in many departmental and institutional committees as a member and the head. He served as the director of the internship program to send interns to oil and gas-related companies. During his deanship of the college or arts and sciences, he initiated programs to support freshmen to be productive university students and developed the curriculum to enhance the learning process. His research interests include oriented around autonomous field robots, design, and control, which includes vehicles and drones.

SAJID JAVED received the B.Sc. degree in computer science from the University of Hertfordshire, U.K., in 2010, and the master's and Ph.D. degrees in computer science from Kyungpook National University, Republic of Korea, in 2017. He is currently a Faculty Member with Khalifa University (KU), United Arab Emirates. Prior to that, he was a Research Fellow with KU, from 2019 to 2021, and the University of Warwick, U.K., from 2017 to 2018. His research interests include visual object tracking in the wild, multi-object tracking, background-foreground modeling from video sequences, moving object detection from complex scenes, and cancer image analytics, including tissue phenotyping, nucleus detection, and nucleus classification problems. His research themes involve developing deep neural networks, subspace learning models, and graph neural networks.